RADC-TR-83-31
Final Technical Report
February 1983

METAL-INSULATOR-METAL JUNCTIONS AS SURFACE SOURCES OF INTERMODULATION

Georgia Institute of Technology

T. G. Shands and J. A. Woody

APPROVED FOR PUBLIC RELEASE; DISTRIBUTION UNLIMITED

ROME AIR DEVELOPMENT CENTER
Air Force Systems Command
Griffiss Air Force Base, NY 13441

This report has been reviewed by the RADC Public Affairs Office (PA) and is releasable to the National Technical Information Service (NTIS). At NTIS it will be releasable to the general public, including foreign nations.

RADC-TR-83-31 has been reviewed and is approved for publication.

APPROVED:

ROY F. STRATTON
Project Engineer

APPROVED:

ROBERT W. MCGREGOR
Acting Chief, Reliability & Compatibility Division

FOR THE COMMANDER:

JOHN P. HUSS
Acting Chief, Plans Office

If your address has changed or if you wish to be removed from the RADC mailing list, or if the addressee is no longer employed by your organization, please notify RADC (RBCT) Griffiss AFB NY 13441. This will assist us in maintaining a current mailing list.

Do not return copies of this report unless contractual obligations or notices on a specific document requires that it be returned.

UNCLASSIFIED

SECURITY CLASSIFICATION OF THIS PAGE (When Data Entered)

REPORT DOCUMENTATION PAGE		READ INSTRUCTIONS BEFORE COMPLETING FORM
1. REPORT NUMBER RADC-TR-83-31	2. GOVT ACCESSION NO.	3. RECIPIENT'S CATALOG NUMBER
4. TITLE (and Subtitle) METAL-INSULATOR-METAL JUNCTIONS AS SURFACE SOURCES OF INTERMODULATION		5. TYPE OF REPORT & PERIOD COVERED Final Technical Report Sep 80 - Nov 82
		6. PERFORMING ORG. REPORT NUMBER N/A
7. AUTHOR(s) T. G. Shands J. A. Woody		8. CONTRACT OR GRANT NUMBER(s) F30602-81-C-0268
9. PERFORMING ORGANIZATION NAME AND ADDRESS Georgia Institute of Technology Engineering Experiment Station Atlanta GA 30332		10. PROGRAM ELEMENT, PROJECT, TASK AREA & WORK UNIT NUMBERS 62702F 23380421
11. CONTROLLING OFFICE NAME AND ADDRESS Rome Air Development Center (RBCT) Griffiss AFB NY 13441		12. REPORT DATE February 1983
		13. NUMBER OF PAGES 90
14. MONITORING AGENCY NAME & ADDRESS(if different from Controlling Office) Same		15. SECURITY CLASS. (of this report) UNCLASSIFIED
		15a. DECLASSIFICATION/DOWNGRADING SCHEDULE N/A

16. DISTRIBUTION STATEMENT (of this Report)

Approved for public release; distribution unlimited.

17. DISTRIBUTION STATEMENT (of the abstract entered in Block 20, if different from Report)

Same

18. SUPPLEMENTARY NOTES

RADC Project Engineer: Roy F. Stratton (RBCT)

19. KEY WORDS (Continue on reverse side if necessary and identify by block number)

Metal-Insulator-Metal Junctions
Intermodulation Products
Measurement Techniques
Interference
Electromagnetic Compatibility

20. ABSTRACT (Continue on reverse side if necessary and identify by block number)

This program was performed to investigate metal-insulator-metal (MIM) junctions as surface sources of intermodulation (IM) on Command, Control, Communications, and Intelligence (C^3I) aircraft. The IM levels generated by MIM junctions were evaluated for various material and physical parameters of the junctions as well as electromagnetic properties of the applied signals. A total of 57 test samples were fabricated to be representative of MIM junctions which are found on aircraft. The IM

DD FORM 1 JAN 73 1473 EDITION OF 1 NOV 65 IS OBSOLETE

UNCLASSIFIED

SECURITY CLASSIFICATION OF THIS PAGE (When Data Entered)

levels of these junctions were measured using a previously developed measurement scheme. Models were developed which describe the IM behavior as a function of some of the parameters. These parameters include input power, temperature, pressure, material and construction of the MIM junction. The changes due to other parameters were smaller than the variability of the data for a single test sample. In order to verify the model, two additional test samples were constructed, measured, and compared to predicted values.

PREFACE

The work described in this report was performed by personnel of the Electronics and Computer Systems Laboratory (ECSL) of the Georgia Tech Engineering Experiment Station. This program was sponsored by the United States Air Force (AFSC), Rome Air Development Center (RADC) as Contract No. F30602-81-C-0268. The program was monitored by Dr. R. Stratton of RADC. The described work was directed by Mr. J. A. Woody, Project Director, and Mr. T. G. Shands, Assistant Project Director, under the technical supervision of Mr. H. W. Denny, Chief of the Electromagnetic Compatibility Division. This report summarizes the objectives, activities, and results of an investigation to study and characterize intermodulation products generated in metal-insulator-metal junctions.

The authors wish to express their appreciation to Mr. David A. Kaiser for his dedicated technical efforts toward completing this project.

TABLE OF CONTENTS

LIST OF FIGURES

LIST OF TABLES

1.0 INTRODUCTION

1.1 Background

Intermodulation products (IMPs) are spurious frequency signals generated by nonlinear components and devices. Particularly in multiple signal environments like those encountered on Command, Control, Communications, and Intelligence (C^3I) aircraft, IMPs generated in nonlinearities may seriously degrade system performance. The extent of system degradation from nonlinearly-generated spurious signals is related to the properties of the nonlinearities, the amplitude of the applied signals, and the relative susceptibility of potential receptors. The magnitude and frequency of the IMPs are related to the voltage transfer characteristic of the particular component and the magnitude and frequency of the injected signals.

The transfer characteristic between the input voltage, e_i, and the output voltage, e_o, for a component is typically expressed as:

$$e_o = A_1 e_i + \sum_{n=2}^{\infty} A_n e_i^n \tag{1}$$

where the A's are constants whose values are dependent upon the properties of the component. The first term of Equation (1) expresses the linear (desired) transfer function of the component. The subsequent series of terms arise from nonlinearities in the transfer function. These "nonlinear" terms provide a measure of the interference-producing properties of the component. They indicate the degree to which intermodulation and spurious response products may be produced, the degree to which distortion and saturation may occur, the degree to which cross modulation may result, etc.

For example, consider the case where the input signal consists of two frequency components such as:

$$e_i = V_1 \cos(2\pi f_1 t) + V_2 \cos(2\pi f_2 t) \tag{2}$$

From Equation (1), the output signal will be:

$$e_o = A_1 V_1 \cos(2\pi f_1 t) + A_1 V_2 \cos(2\pi f_2 t) + \sum_{n=2}^{\infty} A_n \left[V_1 \cos(2\pi f_1 t) + V_2 \cos(2\pi f_2 t) \right]^n \quad (3)$$

Expansion of the infinite summation term indicates that IMPs are generated at frequencies described by the IMP equation:

$$f_{mn} = \pm mf_1 \pm nf_2 \quad (4)$$

where m and n are positive integers which denote the various harmonics of f_1 and f_2 and the sum (m + n) defines the order of the IMP.

Comprehensive research has been conducted on the nonlinear characteristics of active devices such as transistors, diodes, integrated circuits, and other semiconductor PN junctions [1], [2], [3]. For such devices, it has been shown analytically and experimentally that the power relationship between the level of the extraneous IMPs generated and the levels of the two fundamental input signals is:

$$P_{mn} = mP_1 + nP_2 - 2(TOI) \quad (5)$$

where P_1 = power in dBm of the input signal at f_1,
P_2 = power in dBm of the input signal at f_2,
P_{mn} = power in dBm of the IMP at f_{mn} (see Equation (4)), and
TOI = the third order intercept point in dBm which remains a constant value for each device.

In operational situations where high power sources coexist with sensitive receivers, even seemingly inefficient, i.e., weak, IMP generators may lead to serious interference problems. In fact, recent evidence indicates that "passive" components may be sufficiently nonlinear to produce IM interference [4 - 13]. Examples of passive components that are potential IMP generators include metal-insulator-metal (MIM) junctions [14], [15] and coaxial cables and connectors [16], [17].

The generation of IMPs in passive devices arises from the fact that most metals in air intrinsically possess a thin layer of insulation. This insulation results from oxidation, from the presence of foreign impurities on the metal, and from metal treatment processes. When two metallic bodies are joined (as in the case of metal panels on aircraft surfaces) a metal-insulator-metal interface is thus produced. Under the proper set of conditions, this interface is capable of generating IMPs. It may be expected that the IMP levels will be influenced by the types of materials (metals) involved; the metal's surface state, (e.g., presence of coatings or platings, roughness, pressure); the type of junction (e.g., riveted, bolted, welded, etc.), which will affect the contacting area and pressure; environmental factors (temperature and humidity); applied power level (as illustrated by Equation (5)); and frequency.

The IMP levels and their relation to various causative parameters have recently been determined for typical coaxial cable-connector combinations employed on C^3I aircraft [18]. However, these levels and relationships for representative MIM junctions on aircraft have not been previously investigated. On all aircraft, there exist numerous MIM junctions due to the interfaces between the various metal panels which form the exterior surfaces of the aircraft. As more and more sensitive receivers and high power transmitters are placed on the same C^3I platforms, the potential for nonlinear interference becomes more pronounced and harder to avoid. Therefore, to permit prediction and analysis of IMPs resulting from nonlinearities in MIM junctions on C^3I aircraft, more accurate definitions of the potential IMP levels and their relation to the various junction parameters are required. This program was conducted to investigate these relationships.

1.2 Program Scope and Objectives

The scope of this program involved the investigation of passive MIM junction sources of IMPs which cause, or are likely to cause, interference to actual Air Force airborne C^3I systems. Of specific concern were any MIM junction IMP sources (except for antennas) which receive their energy from electromagnetic radiation and which in turn reradiate the IMP energy.

The objective of this effort was to study and characterize the possible MIM junction IMP sources which affect the reception of weak signals by

aircraft C^3I systems in the frequency range of 3 MHz to 10 GHz. The characterization of the IMP source should define the IMP signal as a function of the input signals and the physical specifications of the MIM junction.

1.3 Program Approach

To accomplish the above objective, a 12-month analysis and measurement program was conducted. Initially, the approach was to develop a model based on quantum electron tunneling theory to characterize possible MIM junction IMP sources. After an in-depth literature review and a detailed analysis, it was concluded, however, that an empirical approach was necessary, and the best method, for achieving the stated program objective. Thus, a number of typical MIM junction test samples were fabricated and their IMP levels were measured. The resulting data were analyzed and a model was developed to characterize MIM junction IMP sources.

Finally, two test samples were selected, fabricated, and measured to assess the resulting model.

2.0 THEORETICAL APPROACH

2.1 Electron Tunneling Model Analysis

In order to predict the IMP levels generated by MIM junctions on board C^3I aircraft, an analytical model based on quantum electron tunneling theory was investigated. This theory states that electrons can "tunnel" through a classically forbidden region such as a thin aluminum oxide insulating layer between two aluminum conductors. The current across this insulator, however, has a nonlinear relationship to the applied voltage. It is this nonlinear current-voltage (I-V) relationship that results in the IMP.

Many theoretical investigations have been conducted to derive a nonlinear I-V relationship from electron tunneling theory [19 - 26]. The theory states that the wave function of an electron traveling through a MIM junction matches at the junction boundaries, as indicated in Figure 1. In the tunneling (insulating) region the wave function decreases exponentially, but remains relatively large if the insulator is thin enough. Therefore, in the second conducting region there is a probability for an electron to have "tunneled" through the insulator from the first conducting region.

The WKB approximation [27] can be used to calculate the probability of an electron tunneling through the trapezoidal potential barrier shown in Figure 1. Neglecting temperature effects and the image force potential, the equation describing the tunneling current density J for the trapezoidal potential can be shown to be [21]:

$$J = \frac{me}{2\pi^2\hbar^3}\left[eV\int_0^{E_{F_1}-eV}\exp\left\{\frac{-8m}{3\hbar}\left(\frac{S}{eV+\Delta\phi}\right)\right\}\left[(E+\phi_0+eV+\Delta\phi)^{3/2}-(E+\phi_0)^{3/2}\right]\right\}dE + \int_{E_{F_1}-eV}^{E_{F_1}}(E_{F_1}-E)\exp\left\{\frac{-8m}{3\hbar}\left(\frac{S}{eV+\Delta\phi}\right)\right\}\left[(E+\phi_0+eV+\Delta\phi)^{3/2}-(E+\phi_0)^{3/2}\right]\right\}dE\Bigg] \quad (6)$$

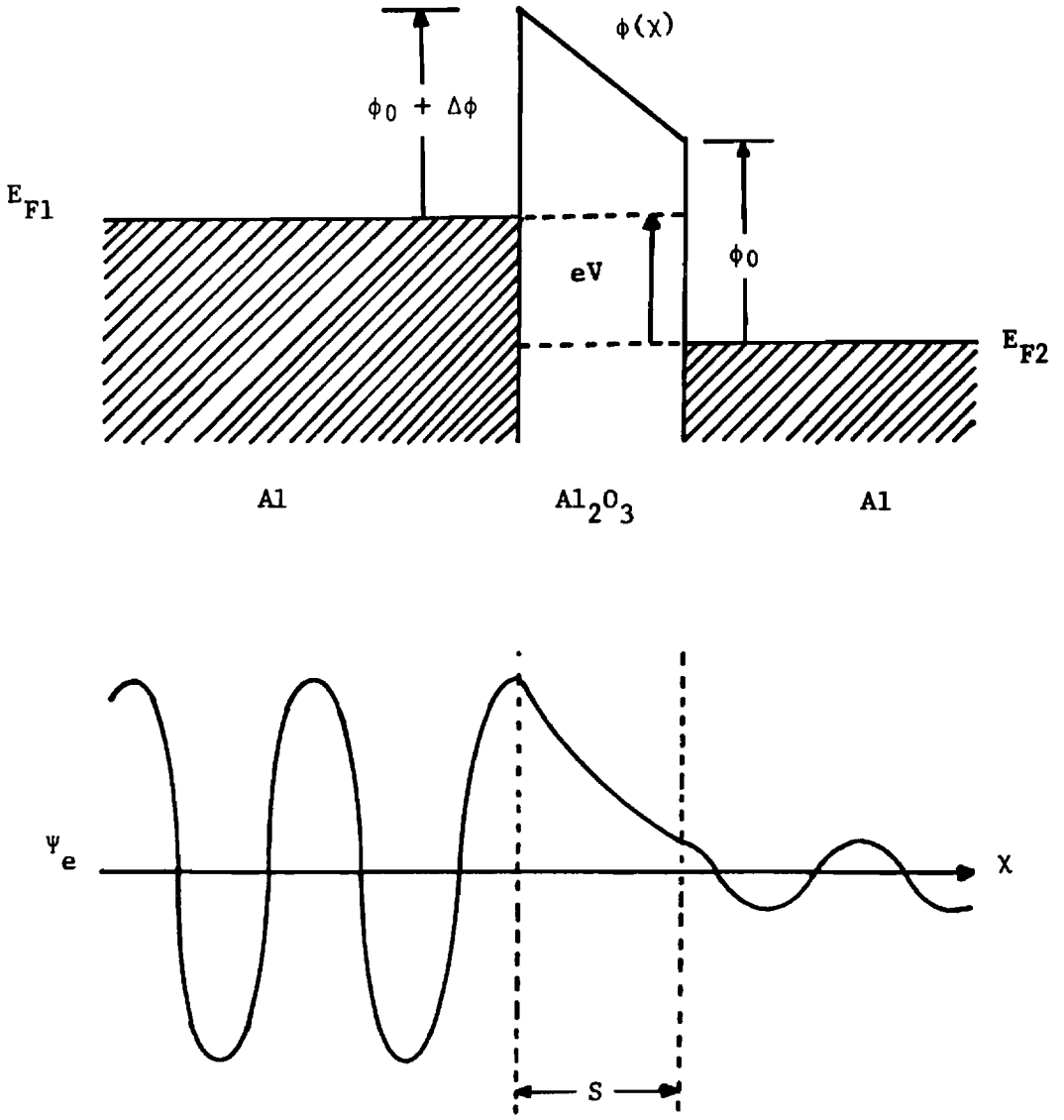

Figure 1. Electron Tunneling through the Potential Barrier of an Insulating Film between two Conductors.

where m = mass of an electron,

e = charge of an electron,

$\hbar$ = Planck's constant divided by 2π,

V = applied potential between 2 conductors,

E_{F_1} = Fermi level in conductor 1,

$\Delta\phi$ = the difference in interface potentials,

E = energy of electron perpendicular to the interface,

ϕ_0 = height of the potential barrier, and

S = thickness of the potential barrier.

Since the trapezoidal potential is the simplest approximation to the actual potential barrier shape and since temperature and image forces are ignored, Equation (6) is the simplest equation for calculating the I-V relationship. However, even this equation is difficult to solve exactly. Therefore, several methods have been used to approximate its solution. Forlani and Minnaja [21] expanded the argument of the exponential about the average of the Fermi levels, while Stratton [22] expanded this argument about the higher Fermi level. Still others have used different approximations, all of which resulted in different forms of the I-V relationship.

Even if a "best" solution were found for Equation (6) there are other limitations to the theory. The equation is derived, and the results are only valid, for a constant potential. No consideration is given to the effects of an alternating potential with a frequency in the 3 MHz to 10 GHz range. Questions also exist as to the applicability of using such macroscopic parameters as the dielectric constant for an insulator that is only a few angstroms thick. Surface roughness, pressure variations, contaminants, and even shorts through the insulator surely have a large effect on the amplitude of the generated IMP levels. In order to consider the effects of these parameters, an equation for tunneling current density would have to be derived using a three-dimensional model instead of the one-dimensional model of Figure 1. Obviously, the complexity of the problem increases rapidly when the parameters and characteristics of realistic MIM junctions in actual environments are considered.

Much experimental research has also been done [28 - 34] to measure the nonlinear I-V relationship and the IMP levels generated in MIM junctions. The MIM junctions constructed for this research, however, have all been highly idealized. Each parameter has been accurately determined using standard metal evaporation and controlled oxidation techniques. These junctions bear as little resemblance to real MIM junctions found on an aircraft as Equation (6) bears to a realistic I-V equation. Yet, even the experimental results from these idealized junctions are not accurately predicted by the electron tunneling models. The measured I-V curves at dc are only approximately similar to those predicted. Also, using the measured I-V curve to calculate IMP levels gives results which can be orders of magnitude different from the measured IMP levels [28].

One must conclude, and most researchers agree, that contemporary electron tunneling theory cannot realistically predict IMP levels produced by MIM junctions on aircraft in actual working conditions. At best a model might be developed which predicts IMP levels on idealized MIM junctions.

2.2 Conclusions

As a result of the in-depth literature review and the preceding analysis of electron tunneling theory, it was concluded that a MIM junction model based on this theory would be inadequate for the following reasons:

- Much research has already been done in this area with large disagreements as to the correct form of the tunneling equations.
- Current state-of-the-art tunneling theory can only predict I-V curves at dc with no frequency dependence.
- Measured I-V curves on carefully controlled idealized MIM junctions, even at dc, are not accurately represented by contemporary electron tunneling models.
- Due to the large number of variables in typical (real-world) MIM junctions and to the inherent instability of the phenomenon, it is the opinion of most researchers that an electron tunneling model cannot predict IMP levels on C^3I platforms.
- If an electron tunneling model were developed, it would at best predict IMP levels only for idealized MIM junctions where each parameter was carefully controlled and measured.

3.0 MEASUREMENT APPROACH

3.1 Introduction

Based on the conclusions in the previous section, a measurement approach to MIM junction modeling was pursued. It was decided that such an approach would provide a higher probability of developing an accurate model and also establish a data base for future efforts. Therefore, model development efforts were directed to the following tasks:

- Construct a variety of MIM junctions which closely resemble aircraft panels, parallel industrial construction techniques, and include different junction parameters. These parameters are the number of rivets, types of rivets, types of metal, thicknesses of metal, chemical treatments, paint primers, and sealants.
- Perform measurements on the test samples to determine the effects of the different junction parameters on IMP generation.
- Perform measurements on a selected number of test samples to determine the effects of such external parameters as vibration, temperature, pressure, input power, and frequency on IMP generation.
- Measure the IMP levels on at least one panel removed from an aircraft to provide a comparison with test sample data.
- Within existing program constraints, model as many reliable relationships between measured IMP levels and the selected parameters as possible.

3.2 Test Samples

In order to design the test samples, an aircraft company, Lockheed-Georgia, was consulted to define typical aircraft construction practices and materials. It quickly became apparent that an extremely large number of junctions with different parameters exist on an aircraft. Furthermore, the construction techniques and the materials vary between different companies and even between different aircrafts manufactured by the same company. In order to establish a realistic bound on the number of junctions to be constructed and tested, test samples were selected to represent typical MIM junctions on the surfaces of aircraft fuselage and wings (these junctions are considered to be the most probable sources of IMP generation on aircraft structures). The test samples were constructed with variations in those

junction parameters considered to be of major concern in IMP generation. Those parameters are as follows:

- o rivet patterns (number and location)
- o rivet type
- o metal type (alloy type)
- o metal thickness
- o chemical treatment
- o metal primer
- o sealant

A total of 57 test samples as identified in Appendix A were chosen to be evaluated.

The construction of the test samples paralleled closely that of industry. First, the surfaces of the aluminum alloys were cleaned. The metal was then treated with a chemical process that placed a coating or an oxidation layer on the surface. Next, the metal was sprayed with a paint primer. Finally, the rivet holes were drilled, a sealant was spread over the surfaces, and the panels were riveted together. Some test samples were more idealized in that they did not contain one or more of the above steps or parameters or were constructed in a special manner. This made it possible to determine the effect of some parameters in the absence of others. For example, some panels were riveted together without a sealant, one was cut from a KC-135 aircraft panel, and others were solid pieces of metal without a junction.

The test samples were usually constructed from three pieces of metal: two of which are 4.75 inches long by 1.5 inches wide while the third is 5.25 inches long by 1.5 inches wide. The two shorter pieces were placed end to end with the longer one overlapping and forming the junction as shown in Figure 2. The test sample was then placed inside a shielded box (test jig). The test sample was positioned the correct distance above a ground plane to insure a characteristic 50-ohm impedance.* The ends of the test sample were soldered

* Measurements indicate that the test sample/test jig combination must match the 50-ohm characteristic impedance of the remainder of the test setup or the measured data will be inaccurate. A VSWR of 1.5:1 can change the measured IMP level by as much as 10 dB compared to a VSWR of approximately 1:1.

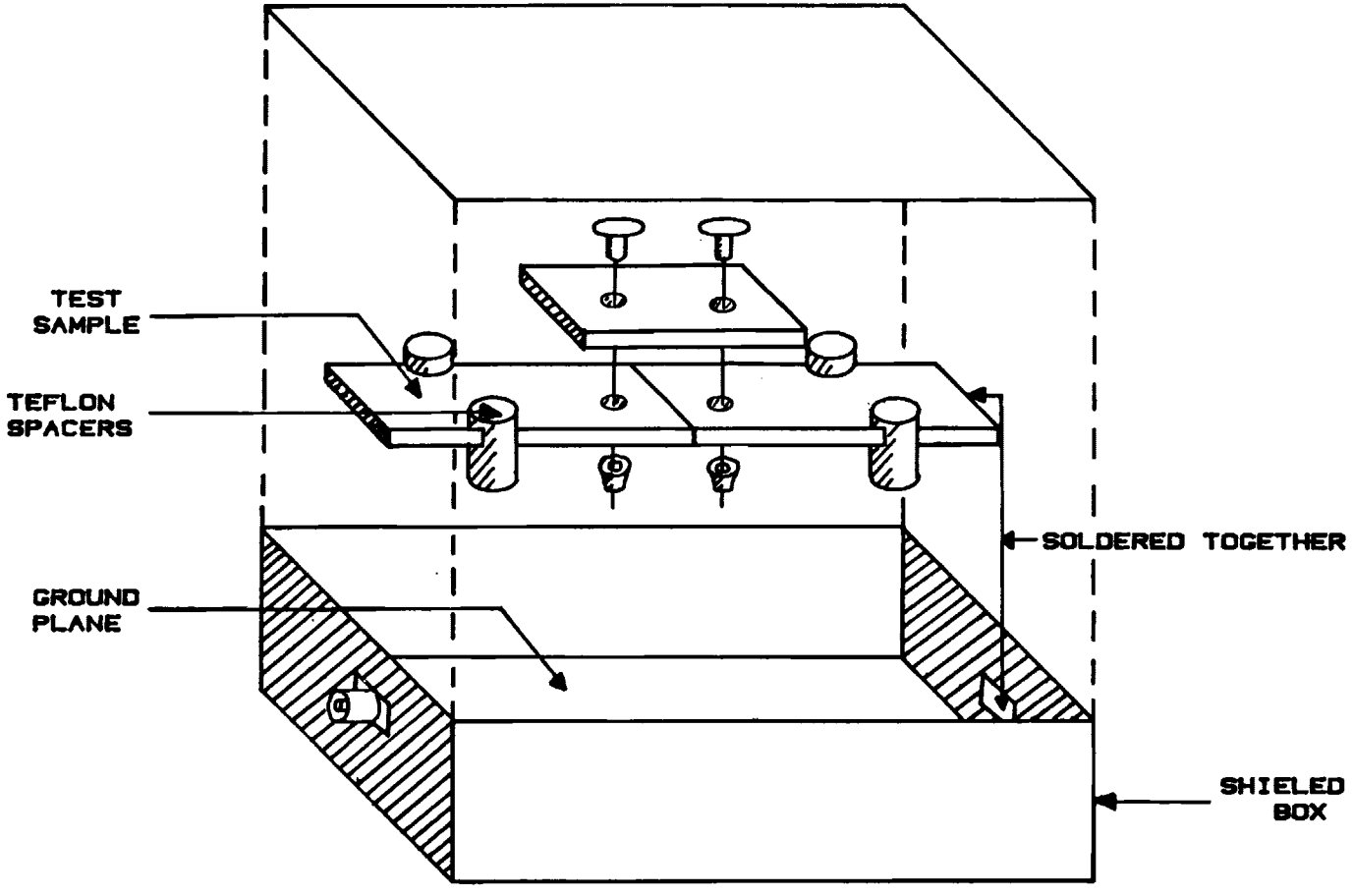

FIGURE 2. TEST SAMPLE WITH TEST JIG.

with an ultrasonic soldering iron to two Type N connectors mounted on the test jig. The ultrasonic soldering iron removes the oxide layers from the surfaces so that the solder can bond the test sample to the connector without forming a MIM junction.*

3.3 IM Measurements

The general block diagram for the measurement test setup is shown in Figure 3 (further details are given in Appendix B). As shown in this figure, two fundamental signals, one at 375 MHz and the other at 400 MHz, are combined such that an input power level** of +44 dBm is applied to the test sample. The signals then pass through the test sample and are terminated in a 50-ohm load. Signals from the test sample are coupled off at a reduced level and examined with a spectrum analyzer for third order IMPs at 350 MHz.

This measurement scheme was developed and evaluated on a recent RADC sponsored research effort to measure the levels of IMPs generated in coaxial cables and connectors [18]. A measure of the repeatability of the test setup at that time showed that over 90% of the IMP measurements were repeatable within 3 dB, over 80% within 2 dB, and over half within 1 dB. The repeatability of the test setup was re-evaluated for the current program with test samples from the previous program. The results were the same.

The reliability of the test setup in measuring the actual IMP levels was also determined. The test setup was carefully calibrated and its sensitivity and inherent (residual) IMP levels measured. The sensitivity, which is simply the noise floor or the minimum measurable signal, was -126 dBm.*** Since the test setup consists of many metal components connected together, it contains a large collection of MIM junctions similar to the test sample. Therefore, the inherent IMP level is the level produced by the test setup when no test sample

---

*The solder used with the ultrasonic soldering iron was proprietary. It is stock number S-100A-XX, manufactured by Fibra Sonics, Inc.

**The input power level is defined as the linear sum of the power levels of the two equal amplitude fundamental signals at the input of the test sample (e.g., an input power of +44 dBm implies that $P_1 = P_2 = +41$ dBm).

***The power levels given in this report for sensitivity and IMPs are the values at the output of the test sample.

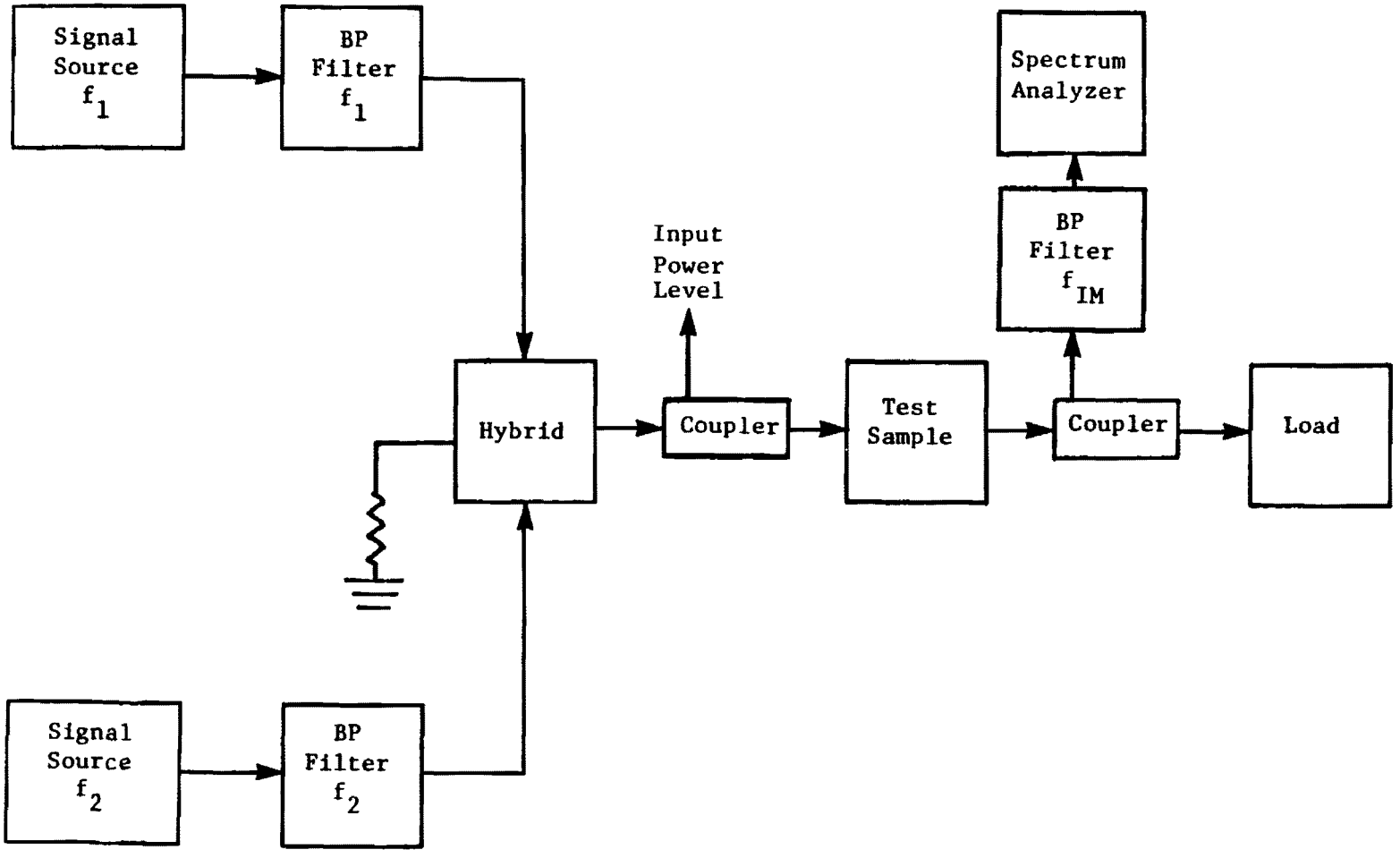

Figure 3. Basic Measurement Setup

is present. This level was reduced to -104 dBm using previously identified techniques and precautions [18]. Such precautions include cleaning the mating surfaces of coaxial connectors and coating them with a conductive grease, carefully threading the connectors and tightening them with hand tools, and rigidly mounting the equipment to reduce vibrations. Finally, a measurement was defined to be valid only if it was $\geq$ 3 dB above the larger of the sensitivity or inherent IMP levels, i.e., $\geq$ -101 dBm.

All 57 test samples were then measured with the test setup (using the procedures described in Appendix C) to determine the effects of junction parameters on IMP generation. Next, the effects of the external parameters were determined. Vibration was applied by simply shaking the test sample. This was done for every test sample and is included in the measurement procedures. Several of the more stable test samples were then selected as controls to determine the effects of the remaining external parameters. The first such parameter was temperature. The temperature of the test sample was increased (or decreased) to a desired level and allowed to return to ambient temperature. The junction temperature was changed by heating with a 200 W soldering iron (or by cooling with a circuit coolant spray). The temperature was monitored with a laboratory grade thermometer. At different temperatures between 9° C and 100° C, the IMP levels were recorded.

The effect of applying an external pressure to the test sample was next determined by monitoring the IMP levels as the test sample was squeezed between two 0.75-inch diameter teflon rods. One rod was placed between the test sample and the ground plane to maintain the correct spacing while a force was applied to the junction with the second rod. The magnitude of the external pressure was varied from 0 to 5 PSI* and measured with a spring scale. To determine the effect of power, the power level of one or both fundamental frequencies was then varied from +26 dBm (.4 watts) to +49.5 dBm (89 watts) as the resulting IMP levels were recorded.

The final external parameter evaluated was frequency. Three test samples were measured at six IMP frequencies between 22 MHz and 1117 MHz. These IMP frequencies and the associated frequencies of the fundamental input

---

* A maximum external force of 39 lbs was applied to the junction which had a cross sectional area of 7.88 in^2.

signals are given in Table 1. Each time frequency was changed, the test setup had to be changed. Details of the test setup for each frequency are discussed in Appendix B. Each test setup was evaluated with respect to repeatability and reliability as described for the basic test setup at 350 MHz. The repeatability results were the same as stated previously. The minimum measurable IMP levels that are valid along with the sensitivity and inherent IMP levels are given in Table 2.

3.4 Data Analysis

3.4.1 Junction Parameters

The measured IMP levels for all of the 57 test samples with a total input power of +44 dBm and a frequency of 350 MHz are recorded in Appendix D and shown graphically in Figure 4. Each "x" in this figure indicates an IMP level which remained stable or constant during its measurement. Each solid line represents an IMP level which was unstable* and varied continuously over a wide range of values during its measurement.

It is clear from Figure 4 that:

- Typical aircraft MIM junctions do produce third-order IMPs which can be relatively large. The IMP levels for the MIM junction test samples ranged over more than 70 dB. (The highest values are as much as 30 dB higher than the highest IMP measured in cables and connectors at the same frequency and input power [18].) The high IMP levels are especially significant when compared with predictions from electron tunneling theory. Most of the surfaces of the metals used to construct test samples were treated chemically and sprayed with a primer so that there is an insulating layer on the order of one mil thick. This is approximately 5000 times too thick for electrons to "tunnel" through [32]. Therefore, according to electron tunneling theory, there should be no measurable IMPs.

*Unstable IMP levels could usually be associated with the vibrations applied to the test sample either on purpose or accidentally. In many cases, very small accidental vibrations caused large variations in the IMP levels. When vibrations ceased, the IMP levels temporarily stabilized at some random level between the extreme values for the range. Stable IMP levels, on the other hand, remained constant even when large vibrations were applied to the test sample. However, measured values of stable IMP levels were not necessarily repeatable.

TABLE 1

IMP TEST FREQUENCIES

IMP Frequency f_{IM} (MHz)	Fundamental Signal Frequencies f_1 (MHz)	f_2 (MHz)
21.9*	19.89*	17.88*
200	250	225
275	250	225
350	400	375
425	400	375
1117.09*	1036.28*	955.47*

*These specific frequencies were selected because of the availability of filters. The IMP frequencies of 21.9 MHz and 1117.09 MHz are referred to in this report by their nominal values of 22 MHz and 1117 MHz, respectively.

TABLE 2

SENSITIVITY LEVELS, INHERENT IMP LEVELS, AND MINIMUM VALID IMP LEVELS OF TEST SETUPS

Nominal IMP Frequency (MHz)	Sensitivity Level (dBm)	Inherent IMP Level (dBm)	Valid IMP Level (dBm)
22	-87	-80	$\geq$ -77
200	-126	-104	$\geq$-101
275	-126	-99	$\geq$ -96
350*	-126	-104	$\geq$-101
350**	-126	-66	$\geq$ -63
425	-126	-70	$\geq$ -67
1117	-100	-78	$\geq$ -75

*These levels are included again for completeness.

**The test setup was changed in order to accommodate input power levels higher than +44 dBm.

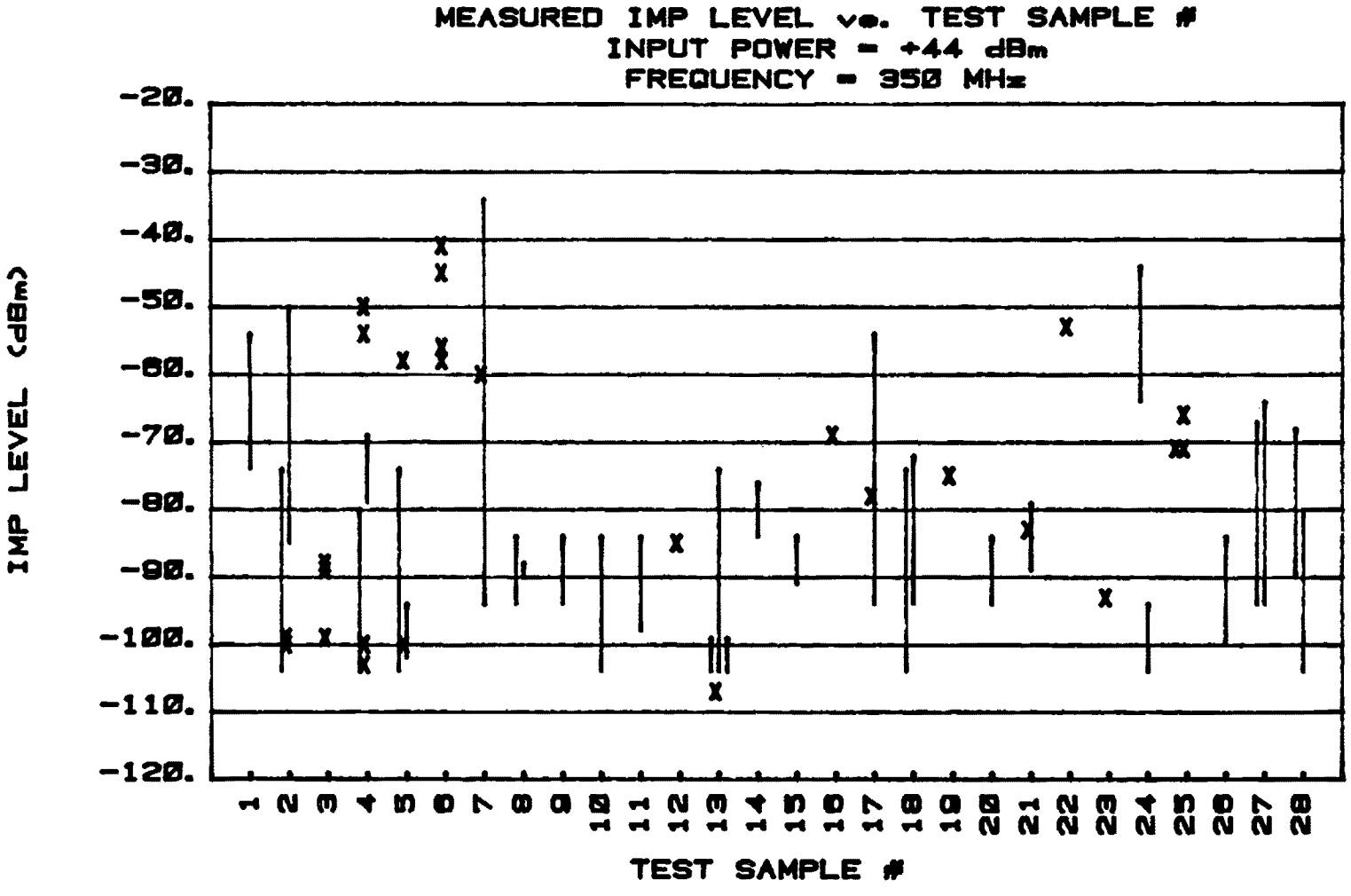

FIGURE 4. MEASURED IMP LEVELS FOR ALL 57 TEST SAMPLES. (CONTINUED)

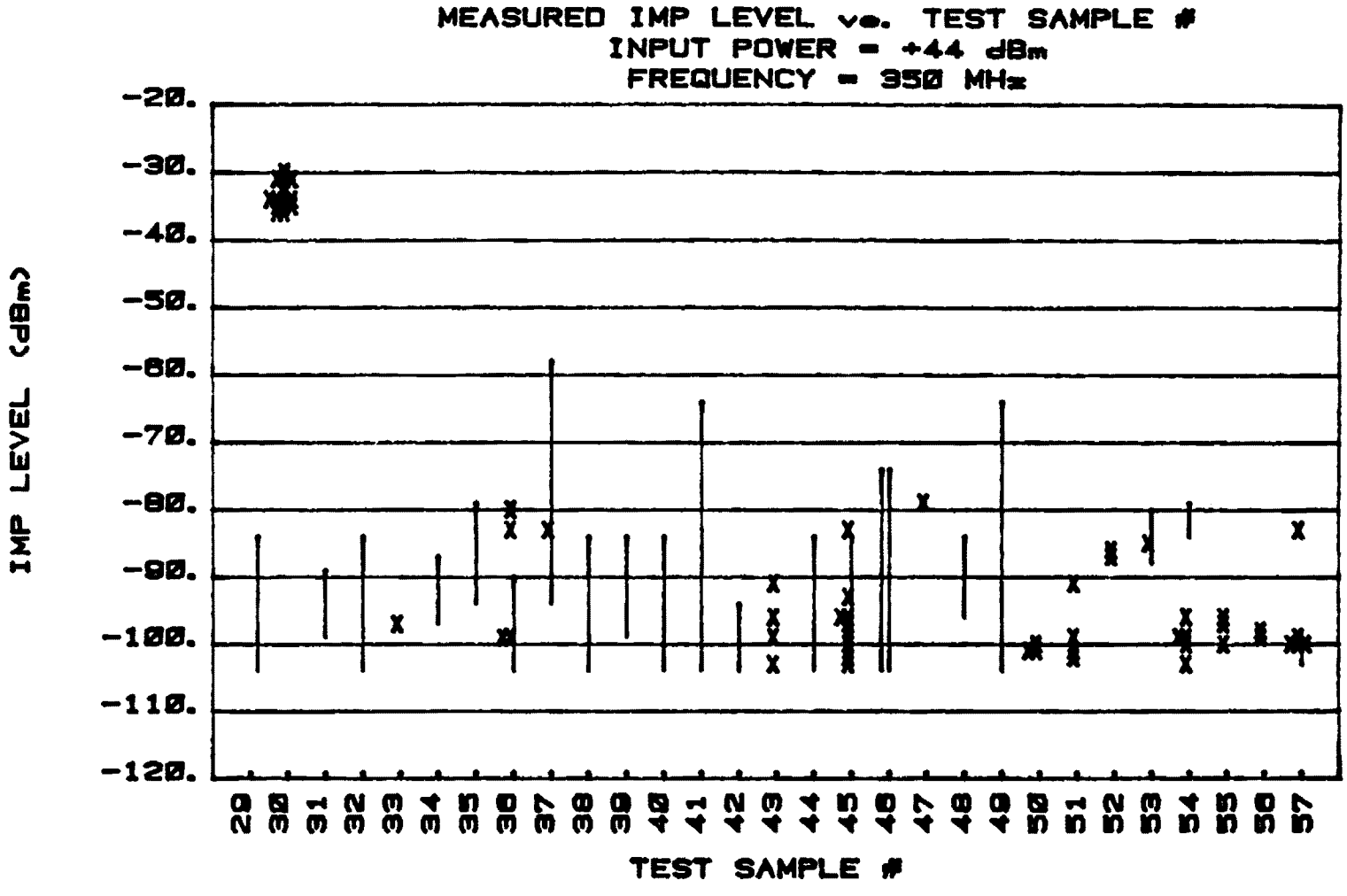

FIGURE 4. MEASURED IMP LEVELS FOR ALL 57 TEST SAMPLES.

- The IMPs produced in a typical aircraft MIM junction are usually very unstable with a wide range of possible values. Of the 57 test samples measured, 40 produced unstable IMP levels with variations as high as 60 dB. Even measurement data on stable IMP levels could generally not be repeated. For example, Test Sample #4 produced 50 dB differences between its minimum and maximum stable levels. Furthermore, some junctions which produced stable levels during one measurement produced unstable levels during another as shown by the data on Test Samples #4, #5, and #7. Yet, others were extremely repeatable such as Test Sample #30 which had 14 measurements falling within $\pm$ 3 dB*.

The specific physical characteristics of each of the samples represented in Figure 4 are listed in Appendix A. An examination of this listing allows the data of Figure 4 to be evaluated for those factors which may be contributing to either the magnitude or the behavior of the IMP characteristic of a particular MIM junction. Individual causative factors can not be identified from Figure 4 alone. However, Appendix A lists the samples according to commonalities in material types, metal thickness, surface treatments, etc. Thus, through a cross matching between the IMP levels of Figure 4 and the junction characteristics of Appendix A, correlations may be attempted.

*One possible explanation for the observed instabilities is as follows: In constructing the test samples, the rivet holes were drilled after all of the surface treatments except sealant were applied. The rivet holes, therefore, penetrated the insulating layers of chemical treatments and primers that are too thick for electrons to "tunnel" through. A sealant was next applied, and rivets were inserted and "riveted". The sealant, however, is a viscous material that can flow between the rivet walls and the rivet, producing an insulating layer that is likely to be nonuniform. In some places the sealant may be thin enough for electron tunneling whereas in others much too thick. Therefore, chance differences in constructing two test samples could have significant effects on IMP generation even though identical materials were used. Some rivets could have a more uniform coating of sealant and produce stable IMPs while others with nonuniform coatings could produce unstable IMPs. Vibration could possibly squeeze the sealant and increase or decrease this nonuniform insulating barrier, resulting in unstable IMP levels. Test samples without sealant, however, would have a very uniform aluminum oxide layer between the rivet walls and the rivet, resulting in relatively stable IMP levels.

For example, Appendix A shows that Samples 1-8 are 2024-T3-A aluminum alloy. All of the samples are 63 mils thick but are subjected to different chemical treatments, metal primers, use of sealants, and number of rivets. Thus, the differences in IMP levels and their relative stabilities may be attributable to these different parameters. For example, Samples 1-3 have no surface treatments and Samples 1 and 2 show widely varying and generally unstable IMP levels, while Sample 3 exhibits repeatable levels. Samples 1 and 2 have a sealant applied and are constructed with single rivets while 3 has no sealant and uses 4 rivets. (No. 3 was also exposed to weathering effects.) Samples 4-8 all use sealant and are constructed with one rivet on each side of the joint. Differing surface treatments are used and the IM levels show even greater variations in behavior than do Samples 1-3. Thus, the results on these eight samples tend to point toward either the sealant or number of rivets as the primary contributors to the IMP level and behavior characteristics of the junction. Unfortunately, they do not permit the causative parameters to be quantified.

Note, that Samples 40-45 are also 2024-T3-A aluminum alloy and are 63 mils thick; they have no surface treatments, do not contain sealants, and are constructed with different numbers of rivets. Figure 4 shows that the measured IMP levels still exhibit mixed characteristics of stable and unstable levels, although the levels are generally lower than those of Samples 1-8. These comparisons tend to suggest that surface treatments are more important than rivets to the junction's IMP behavior.

Samples 15-33 are constructed with single rivets on each side of the joint. Various combinations of surface treatments and use of sealants are represented in these samples. Both stable and unstable product levels are evident in the data. It is difficult to discern which of the surface treatments are responsible for the product characteristics. For example, Sample No. 19 and Sample No. 30 are similarly constructed with a sulfuric acid treatment and both have epoxy polyamide primers, yet the IMP levels are different by 40 dB. No. 23 utilizes a clear conversion coating and epoxy polyamide primer and exhibits a stable IMP level that is about 60 dB less than No. 30. Thus, for similar surface treatments and primers, a wide range in behavior of IMP levels and their stabilities is evident -- some levels are low, some are high, some are stable, and some are unstable.

The type of metal forming the junction is important. For example, consider Samples 50-55. These are non-aluminum samples with no surface treatments and in general, the IMP levels generated by these samples are relatively low and stable.

The examination of the measured IMP behavior in this manner indicates that certain parameters of the junction, namely surface treatments and sealants, exert a stronger influence on the level and stabilities of the products than do other parameters, e.g., rivets. However, it does not permit the influence of a particular parameter to be quantified.

A further evaluation of possible relationships between junction parameters and IMP levels can be done by grouping the various junctions together so as to allow direct comparison of results produced by junctions having only individual differences in their construction. Table 3 represents one such grouping. This arrangement permits the effects of individual parameters to be observed independent of the effects of other parameters. For example, to determine the effects of rivet patterns and numbers on IMP levels, Group #29 (test samples #3, #40, #41, #42, #43, and #44) would be selected.

From an initial review and analysis of the Table 3 data, it is clear that, because of the large variations in unstable IMP levels, it is difficult to identify significant data trends or characteristics from unstable IMP data. For instance, note from Figure 4 that the IMP levels for the test samples in Group #29 have variations between 10 dB and 40 dB. Therefore, the effect of rivet* patterns on IMP levels can hardly be determined unless it

---

*The column "Rivet Type" in Table 3 compares test samples constructed with different types of rivets as well as test samples constructed from a solid piece of metal with no rivets or junctions. In the test samples with junctions there are two possible sources of IMPs. One is the test junction to be measured and the other is the solder junction between the test sample and the test jig. In the test samples without junctions, the only possible source of IMPs is the solder junction. In every case the test samples with no junctions produced lower IMP levels than those with junctions. For example, Test Sample #50 in Group 31 was constructed from a solid piece of copper while Test Sample #51 was constructed from three pieces of copper which were riveted together. Test Sample #50 had an average IMP level which was 5 dB lower than Test Sample #51. Thus, it is concluded that the major source of IMP generation is indeed the test junction and not the solder junction.

TABLE 3

TEST SAMPLE PARAMETER COMPARISON

		TEST SAMPLE PARAMETERS							
							Rivets		
Comparison Group	Test Sample Numbers	Aluminum Alloy Type	Nominal Thickness (mils)	Chemical Treatment	Primer Type	Sealant (yes/no)	Number on Each Side of Junction	Type	IMP Levels (dBm)
1	34	7075-T-6511-X							-97 to -87
	45	2024-T3-A							-95
2	44	2024-T3-A							-104 to -84
	51	Copper							-96
	55	Brass							-99
3	50	Copper							-101
	54	Brass							-100
	56	2024-T3-A							-99
	57	2024-T3-A							-97
4	11	3003-H-14							-98 to -84
	14	6061-T6							-84 to -76
5	10	3003-H-14							-104 to -84
	12	6061-T6							-86
6	9		30						-94 to -84
	10		40						-104 to -84
	11		125						-98 to -84
7	12		40						-86
	13		50						-101
	14		125						-84 to -76

(Continued)

TABLE 3 (Continued)

TEST SAMPLE PARAMETER COMPARISON

Comparison Group	Test Sample Numbers	TEST SAMPLE PARAMETERS: Aluminum Alloy Type	Nominal Thickness (mils)	Chemical Treatment	Primer Type	Sealant (yes/no)	Rivets: Number on Each Side of Junction	Rivets: Type	IMP Levels (dBm)
8	34		63						-97 to -87
	35		100						-94 to -79
9	4			Chromic Acid Anodized					-69
	6			Sulfuric Acid Anodized					-51
	8			Color Conversion Coating					-94 to -84
10	5			Chromic Acid Anodized					-80
	7			Sulfuric Acid Anodized					-61
11	15			Chromic Acid Anodized					-91 to -84
	20			Color Conversion Coating					-94 to -84
	23			Clear Conversion Coating					-94
12	16			Chromic Acid Anodized					-70
	18			Sulfuric Acid Anodized					-104 to -72

(Continued)

TABLE 3 (Continued)

TEST SAMPLE PARAMETER COMPARISON

Comparison Group	Test Sample Numbers	TEST SAMPLE PARAMETERS							IMP Levels (dBm)
		Aluminum Alloy Type	Nominal Thickness (mils)	Chemical Treatment	Primer Type	Sealant (yes/no)	Rivets: Number on Each Side of Junction	Rivets: Type	
12 (Cont.)	21			Color Conversion Coating					-84
	24			Clear Conversion Coating					-104 to -44
13	17			Chromic Acid Anodized					-79
	19			Sulfuric Acid Anodized					-76
	22			Color Conversion Coating					-54
	25			Clear Conversion Coating					-70
14	27			Chromic Acid Anodized					-94 to -64
	32			Color Conversion Coating					-104 to -84
15	28			Chromic Acid Anodized					-104 to -68
	30			Sulfuric Acid Anodized					-35
	33			Color Conversion Coating					-98

(Continued)

TABLE 3 (Continued)

TEST SAMPLE PARAMETER COMPARISON

Comparison Group	Test Sample Numbers	TEST SAMPLE PARAMETERS							IMP Levels (dBm)
		Aluminum Alloy Type	Nominal Thickness (mils)	Chemical Treatment	Primer Type	Sealant (yes/no)	Rivets: Number on Each Side of Junction	Rivets: Type	
16	26			Chromic Acid Anodized					-100 to -84
	37			None					-84
17	29			Sulfuric Acid Anodized					-104 to -84
	31			Color Conversion Coating					-99 to -89
	38			None					-104 to -84
	39			None					-99 to -84
18	4				Zinc Chromate Epoxy Polyamide				-69
	5								-80
19	6				Zinc Chromate Epoxy Polyamide				-51
	7								-61
20	16				Zinc Chromate Epoxy Polyamide				-70
	17								-79

(Continued)

TABLE 3 (Continued)

TEST SAMPLE PARAMETER COMPARISON

Comparison Group	Test Sample Numbers	TEST SAMPLE PARAMETERS: Aluminum Alloy Type	Nominal Thickness (mils)	Chemical Treatment	Primer Type	Sealant (yes/no)	Rivets: Number on Each Side of Junction	Rivets: Type	IMP Levels (dBm)
21	18				Zinc Chromate Epoxy Polyamide				-104 to -72
	19								-76
22	21				Zinc Chromate Epoxy Polyamide				-84
	22								-54
23	24				Zinc Chromate Epoxy Polyamide				-104 to -44
	25								-70
24	27				Zinc Chromate Epoxy Polyamide				-94 to -64
	28								-104 to -68
25	29				None Epoxy Polyamide				-104 to -84
	30								-35
26	31				None Zinc Chromate				-99 to -89
	32								-104 to -84

(Continued)

TABLE 3 (Continued)

TEST SAMPLE PARAMETER COMPARISON

Comparison Group	Test Sample Numbers	TEST SAMPLE PARAMETERS							IMP Levels (dBm)
		Aluminum Alloy Type	Nominal Thickness (mils)	Chemical Treatment	Primer Type	Sealant (yes/no)	Rivets: Number on Each Side of Junction	Rivets: Type	
26 (Cont.)	33				Epoxy Polyamide				-98
27	1					Yes			-74 to -54
	2					Yes			-101
	45					No			-95
28	37					No			-84
	38					Yes			-104 to -84
	39					Yes			-99 to -84
29	3						4		-93
	40						4		-104 to -84
	41						4		-104 to -64
	42						4		-104 to -94
	43						3		-96
	44						1		-104 to -84
30	44							Buck	-104 to -84
	45							Torque	-95
	49							None	-104 to -64
	56							None	-99
	57							None	-97
31	50							None	-101
	51							Buck	-96

(Continued)

TABLE 3 (Concluded)

TEST SAMPLE PARAMETER COMPARISON

Comparison Group	Test Sample Numbers	TEST SAMPLE PARAMETERS							IMP Levels (dBm)
		Aluminum Alloy Type	Nominal Thickness (mils)	Chemical Treatment	Primer Type	Sealant (yes/no)	Rivets: Number on Each Side of Junction	Rivets: Type	
32	52							None	-88
	53							Buck	-86
33	54							None	-100
	55							Buck	-99

makes greater than 10 dB difference. Even then, it is difficult to ascertain whether the effect is due to the rivet pattern or a change in the unstable IMP levels. For this reason, only the stable IMP levels should be used to analyze possible test sample parameter/IMP level relationships. For each test sample, the stable IMP levels are averaged to give one number. These averaged, stable IMP levels are included in Table 3.

An examination of the groupings in Table 3 permits further evaluation of the effects of individual junction parameters to be made. For example,for each comparison of stable IMP levels in Groups 9-17 between test samples that have a chromic acid anodizing treatment and those with a sulfuric acid anodizing treatment, chromic acid anodizing treatments appear to produce lower IMP levels. Also, a comparison of stable IMP levels between samples with different primer types (Groups 18-26) indicates that zinc chromate primer is generally associated with higher levels than is epoxy polyamide. Because the data for certain parameters are limited, the results of this process were inconclusive. Consequently, an alternative approach to the formulation of an expression (i.e., model) describing the behavior of IMP levels with different joint parameters was sought.

The alternate approach was to evaluate the average of the stable IMP levels for test samples that contain the same value for one parameter. If this parameter makes a large change in the IMP levels, then an average of all test samples constructed with one value for that parameter should be different from an average of all test samples with a different value for the same parameter regardless of what other parameters change. Obviously only those parameters that result in gross changes in IMP levels can be discovered in this manner.

With this alternate approach, all of the averaged stable IMP levels for test samples with a chromic acid anodizing treatment were compared to the average of the stable IMP levels for test samples with a sulfuric acid anodizing treatment. The value for chromic acid anodizing treatments was higher than the value for sulfuric acid anodizing treatments, which is a different result than indicated above. Comparison of the product levels exhibited by samples having a zinc chromate primer with those having a epoxy polyamide primer shows that the mean levels are within 1 dB of each other which does not substantiate the previous qualititative observation.

In this manner all of the junction parameters were examined. Except for sealant, either no effect was observed or the effect was found to be small relative to the repeatability of the data. Using a sealant in the test sample construction, however, caused an average increase in IMP levels and the levels showed greater instabilities. The average of the stable IMP levels of all junctions constructed without a sealant was -93 dBm with a standard deviation of 6 dB. The average of the stable IMP levels of junctions constructed in a similar manner, but with a sealant, was -72 dBm with a standard deviation of 18 dB.

In conclusion, these various analyses of the measured data do not yield definitive relationships between the IMP levels and particular joint parameters. The data do show that aluminum joints constructed* like those found on C^3I platforms can be sources of potentially troublesome IM products. The products generated by these joints are indeed shown to be highly variable, both with time and with physical parameters. Unfortunately, the particular causative junction parameters are not clearly evident. Although surface treatments appear to be a strong factor in the behavior of the products, the specific relationships, except for sealant, between product levels and surface treatments can not be defined from the measured data.

3.4.2 External Parameters

The effect of such external parameters as vibration, temperature, pressure, and frequency on IMP generation was next determined. Test Samples #30, #6, and #4 were chosen as controls. Test Samples #30 and #6 were chosen because they were the most stable test samples that produced high IMP levels. Test Sample #4 was chosen as typical of test samples with unstable as well as stable IMP levels and large variations in both.

---

*In order to determine if the constructed test samples and results were indicative of MIM junctions found on actual planes, a panel cut from a KC-135 aircraft was measured. This panel (Test Sample #46) had IMP levels that were unstable and ranged from -74 dBm to -101 dBm. These values were within the range of those for other test samples and typical of most.

The data recorded on Test Sample #30 for temperature versus IMP levels is shown in Figure 5 and given in Appendix D. Two sets of data are shown which were taken at different times. Both data sets show an increase in IMP levels of approximately 1 dB for every 10^{o} C as shown with the straight lines plots. Most importantly, however, the heating seemed to have a permanent effect on IMP generation. When the test sample returned to ambient temperature the IMP level remained stable, but at a different value than before. (If sealant is the primary insulator as suggested, an increase in temperature could cause the sealant to flow resulting in this permanent change in the IMP level.)

Applying an external pressure to Test Sample #30 caused no change in the IMP level. The same result was observed for Test Sample #6. For Test Sample #4, however, a decrease in the IMP level occurred as the external pressure was increased. This variation is qualitively represented in Figure 6. Recall that both Test Samples #30 and #6 had fairly stable and repeatable IMP levels. Test Sample #4, on the other hand, had unstable as well as stable IMP levels, both with large variations. The maximum and minimum values shown in Figure 6 are approximately the same as measured previously for Test Sample #4 with no external pressure. These results suggest that the IMP levels of junctions with unstable levels can be reduced by applying an external pressure, i.e., bonding them more tightly.

Test Sample #30 was also used to determine the effect of the input power levels of each fundamental frequency on IMP generation. Figure 7 and Appendix D give each data point in sequential order. For the points 1 - 10 and 24 - 33 the input power P_2 was kept constant while P_1 was varied. In general the change between these points is approximately a 2 dB increase in IMP level for each 1 dB increase in input power, i.e., a slope of 2. For points 11 - 16 and 34 - 37, the input power P_1 was kept constant while P_2 was varied. The slope between each of these points is approximately 1. Finally, for the points 17 - 23 and 38 - 39, P_1 was kept equal to P_2 and both were varied. The average slope here is 3.

Between the measurements for points 23 and 24, elements of the test setup were changed to accomodate fundamental power levels greater than +41 dBm. As observed on the previous effort [18], this change in the test setup results in unexplained shifts in the measured IMP levels (as much as 30 dB in Figure 7)

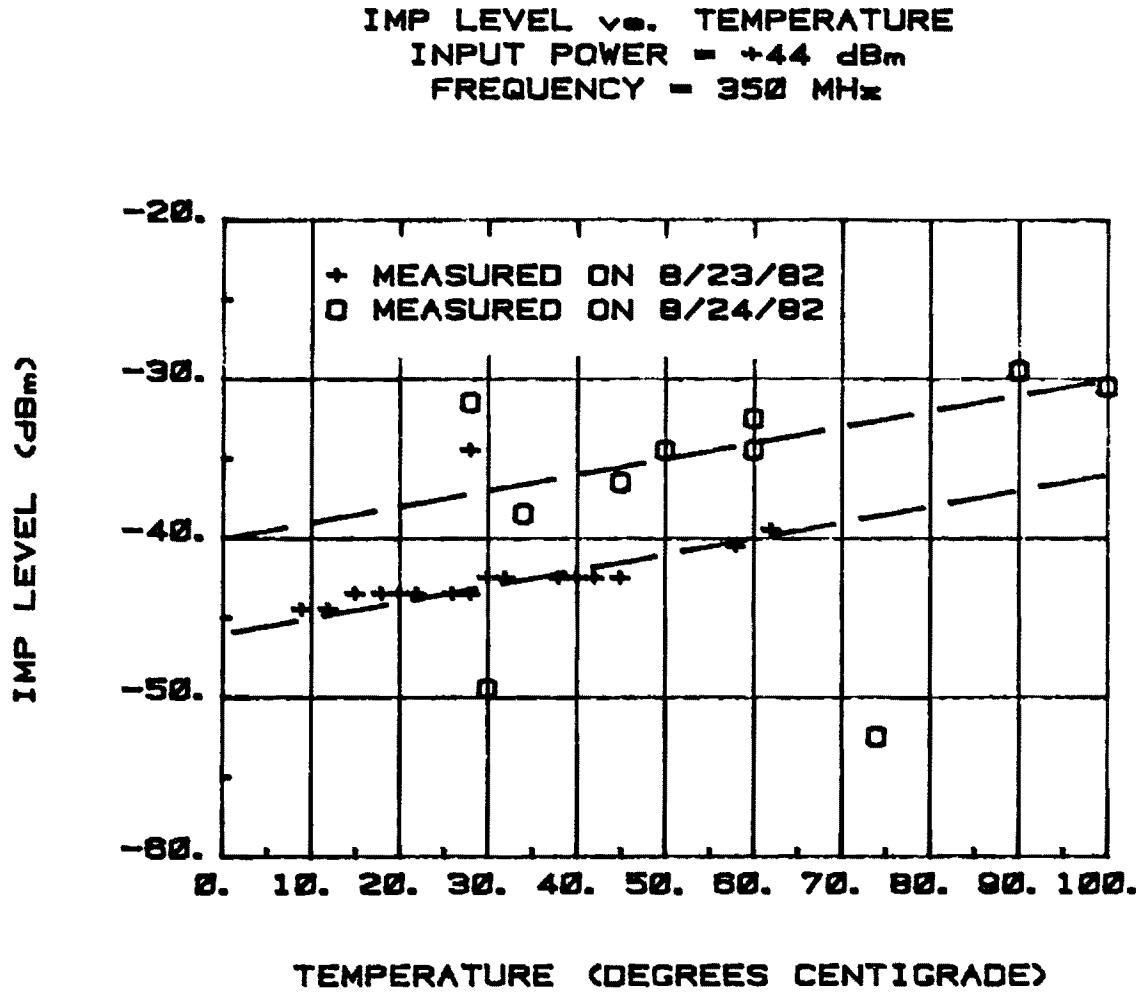

FIGURE 5. IMP LEVEL MEASURED AS A FUNCTION OF TEMPERATURE FOR TEST SAMPLE NO. 30 AND PLOTTED WITH BEST-FIT STRAIGHT LINES.

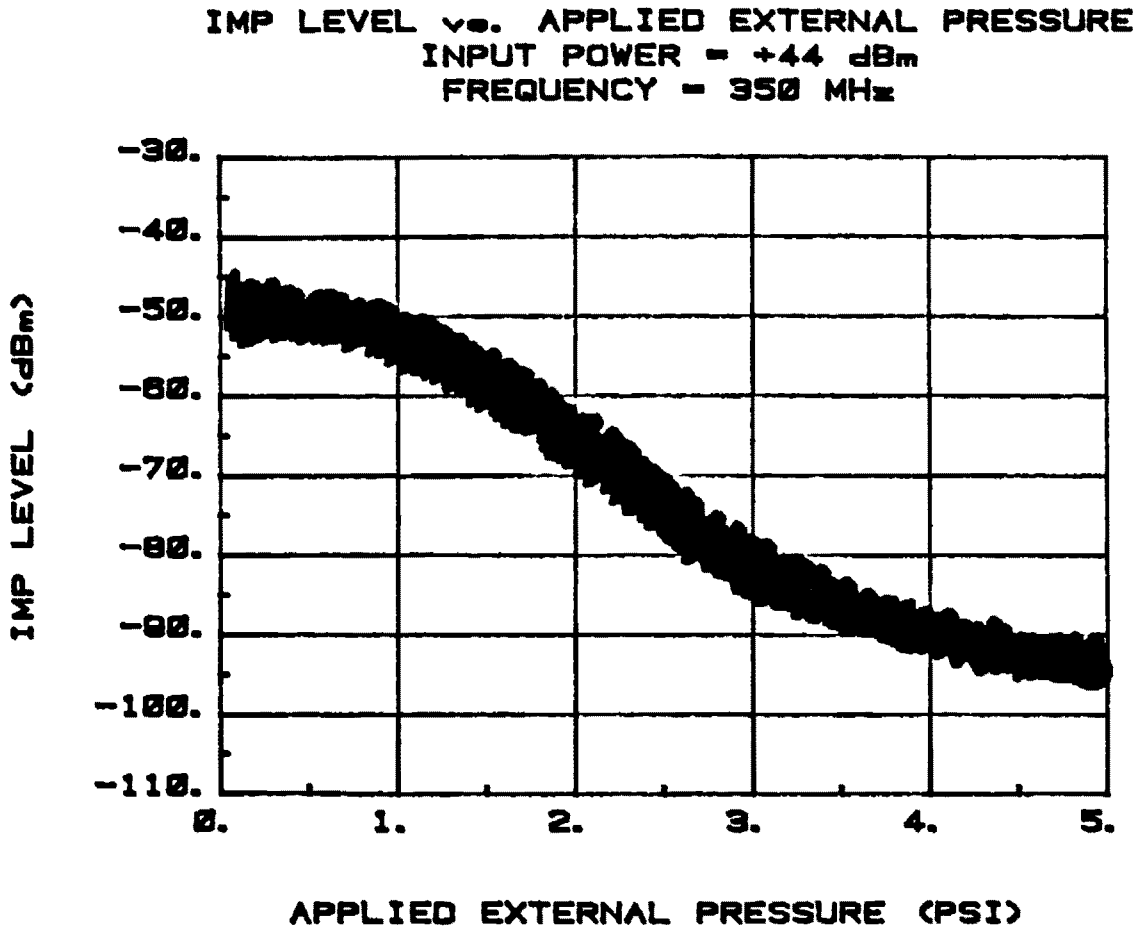

FIGURE 6. IMP LEVEL QUALITATIVELY SHOWN AS A FUNCTION OF APPLIED EXTERNAL PRESSURE FOR TEST SAMPLE NO. 1.

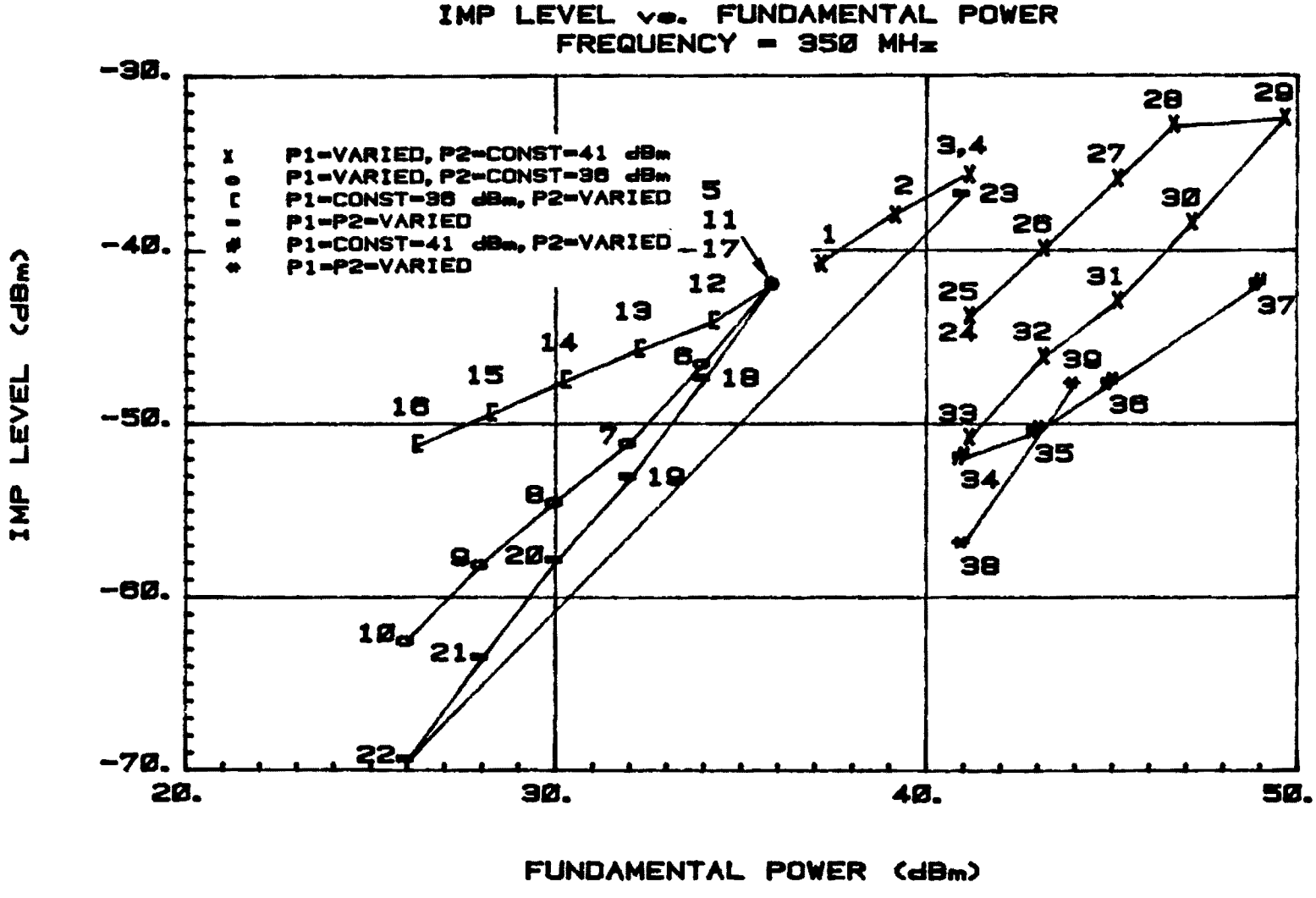

FIGURE 7. IMP LEVELS SHOWN AS A FUNCTION OF FUNDAMENTAL POWER FOR TEST SAMPLE NO. 30.

even for the same fundamental power levels. The other shifts in IMP levels in Figure 7 appear to occur after one of the fundamental power levels is increased above +47 dBm. This observation indicates that large RF power levels may also cause unexplained shifts in the measured IMP levels. (It is noted that the average slopes are the same before and after the shifts.)

Using the average slopes, the level of this particular IMP can be related to the fundamental input powers by:

$$P_{IM} = 2P_1 + P_2 + \text{"X"} \tag{7}$$

where P_{IM} = power in dBm of the IMP at $2f_1 - f_2$,
P_1 = power in dBm of the input signal at frequency f_1,
P_2 = power in dBm of the input signal at frequency f_2, and
"X" = a level in dBm which has been shown to change as much as 30 dB.

The corresponding relationship between IMP levels and fundamental input powers for semiconductor devices has been shown to be [35]:

$$P_{IM} = 2P_1 + P_2 - 2(TOI) \tag{8}$$

where P_1 = power in dBm of the input signal at frequency f_1,
P_2 = power in dBm of the input signal at frequency f_2, and
TOI = the third order intercept point in dBm which remains a constant value for each device.

The MIM junction model (Equation (7)) is similar to the semiconductor model (Equation (8)). The only difference is that the third order intercept in Equation (8) is a constant for each device whereas "X" in Equation (7) can have several values for a single MIM junction. The changes in "X" apparently depend on the components used in the test setup and the maximum power that has been applied to the test sample. As a result of the variable nature of "X", it is difficult, and not considered meaningful, to define the equivalent of a third order intercept for a MIM junction test sample. Although the MIM junction IMP levels increase with the input signal levels in the correct proportions, the data curves tend to be multivalued. Thus, efforts to project

(i.e., model) IMP levels produced at one input power level to those produced at another input power level should be approached with caution.

The final external parameter to be examined is frequency. The IMP levels of Test Samples #30, #6, and #4 versus frequency are shown in Figures 8, 9, and 10, respectively. This data is also recorded in Appendix D. As seen collectively in all the figures, no well ordered relationship is evident. For example, in Figure 8 the frequency behavior of the IMP levels could be described as a constant value of -38 dBm with a $\pm$ 10 dB spread. Figure 9, however, tends to suggest decreasing levels with frequency or perhaps quadratic behavior. The IMP levels shown in Figure 10, on the other hand, can not be described very well because of the erratic behavior of the products. The levels measured at all frequencies between 22 MHz and 1117 MHz fall within the range of levels shown in Figure 4 for 350 MHz. Thus, no clear dependence on frequency was noted for IM products produced by the various junctions.

3.5 MIM Junction Model

C^3I platforms are heavily populated with transmitters and receivers and with MIM junctions. Systems EMI analyses of such platforms depend upon established, quantative relationships, i.e., models, of the various interference sources. Since MIM junctions have indeed been shown to readily produce interference products, a quantative model of junction behavior is highly desirable. Unfortunately, as the previous discussion illustrates, the IM products produced by typical MIM junctions do not exhibit well ordered behavior with the internal factors of rivet numbers, rivet patterns, metal alloy, metal thickness, chemical treatment, metal primer, and sealant. More definitive relationships between IMP behavior and the external factors of temperature, pressure, power of fundamental signals, and frequency were noted. The behavior with pressure proved to be more qualitative than quantitative; the results with frequency were mixed. The results of the temperature tests indicated that IMP levels appeared to increase 1 dB for each 10 degrees change from ambient, or

$$\Delta \text{IMP (dB)} = \frac{T-28}{10} \qquad (9)$$

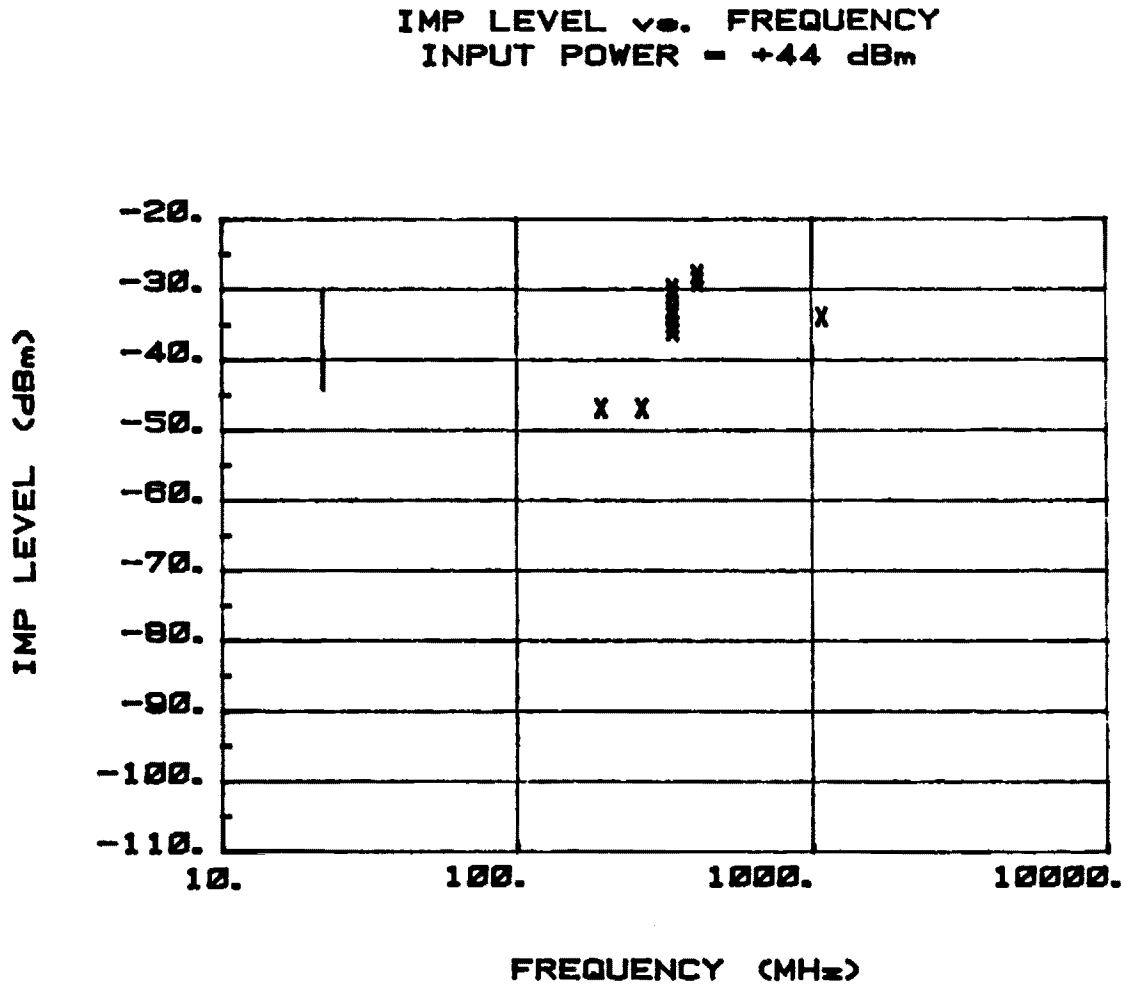

FIGURE 8. IMP LEVEL MEASURED AS A FUNCTION OF FREQUENCY FOR TEST SAMPLE NO. 30.

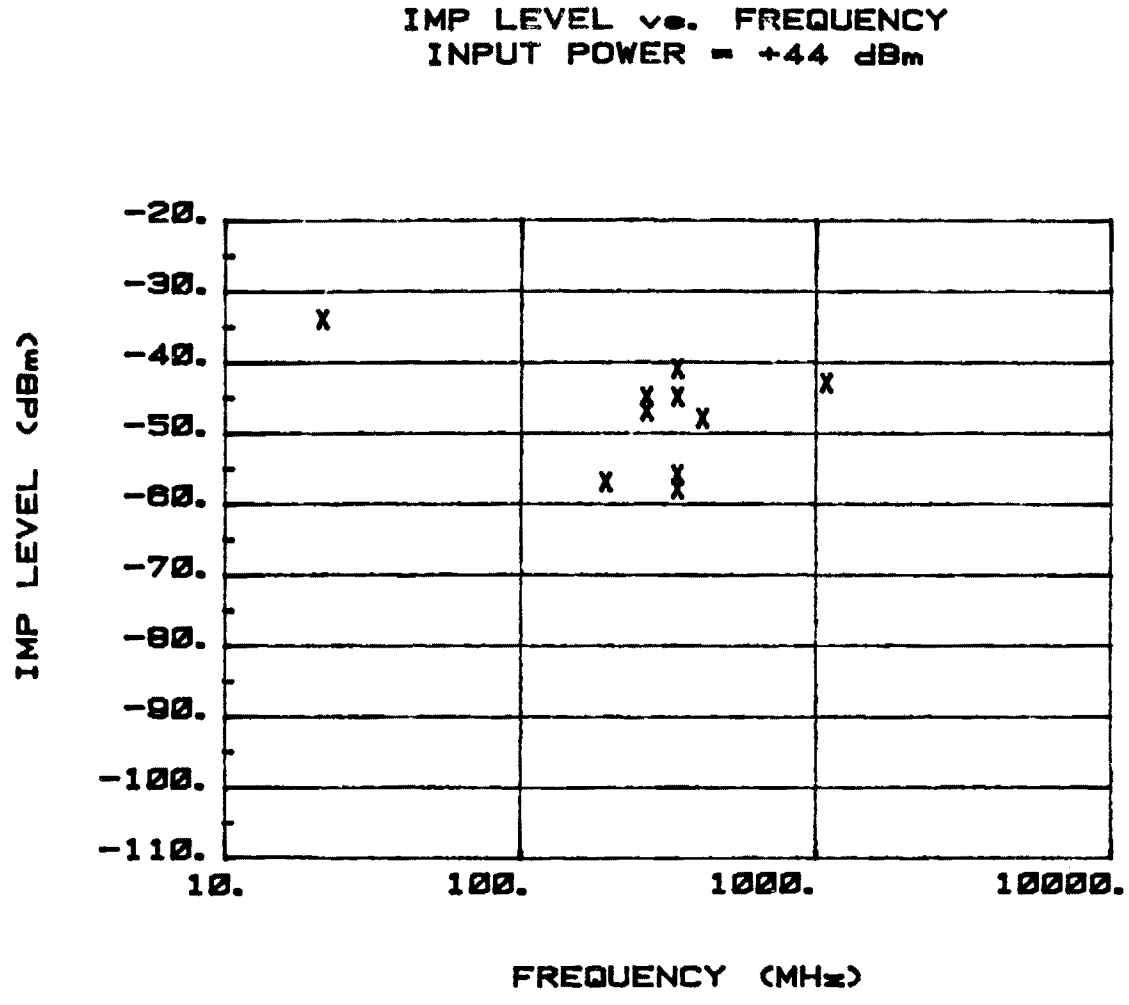

FIGURE 9. IMP LEVEL MEASURED AS A FUNCTION OF FREQUENCY FOR TEST SAMPLE NO. 6.

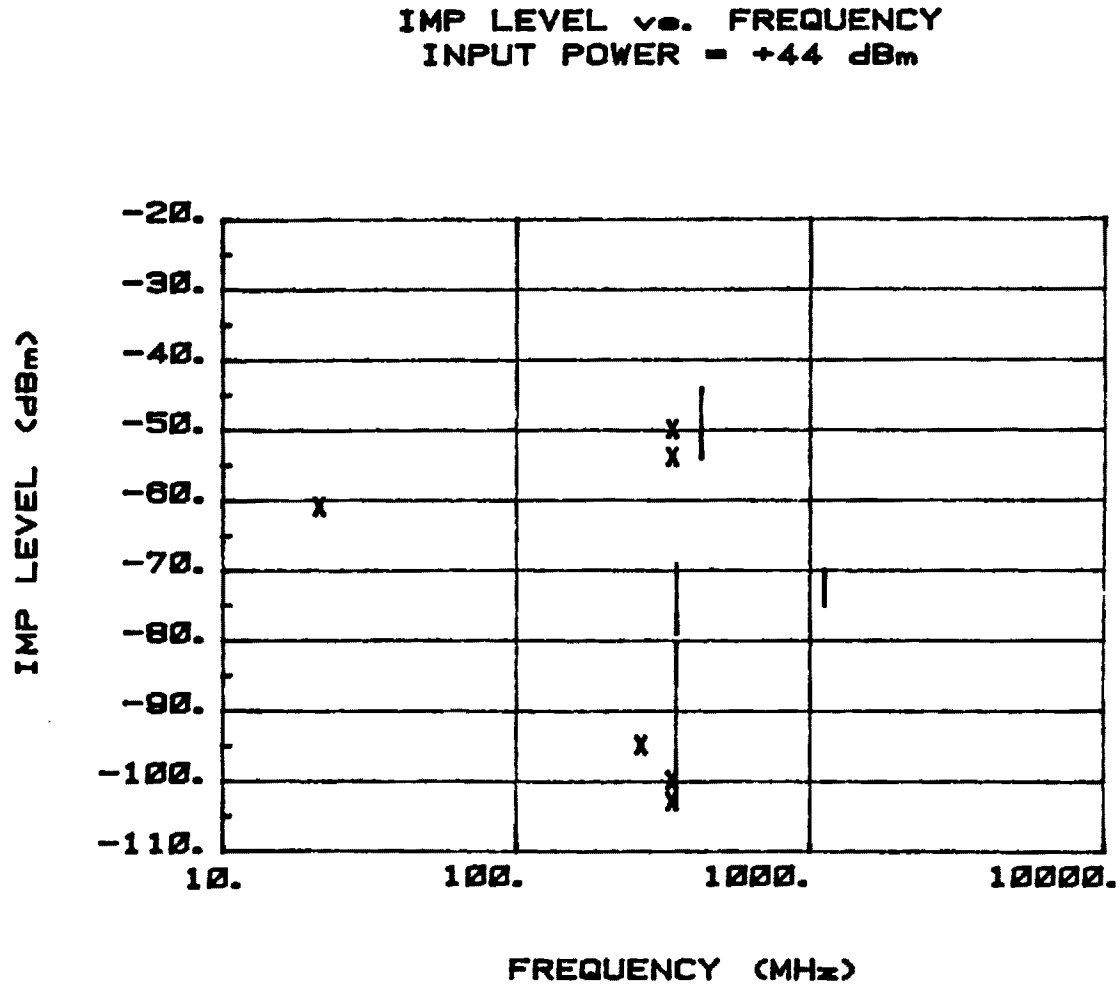

FIGURE 10. IMP LEVEL MEASURED AS A FUNCTION OF FREQUENCY FOR TEST SAMPLE NO. 4.

where T equals the temperature in degrees Celsius of the junction and ambient is equal to 28°C. Intermodulation levels increase with input power according to the harmonic relationship between the IMP and the fundamental signal being increased, i.e., in the classical fashion

$$P_{IM} = mP_1 + nP_2 \tag{10}$$

This behavior must be viewed with caution because of the multivalued behavior of the measured data curves.

Thus, out of the 12 causative factors examined, only two exhibited sufficiently stable behavior to be included in a model. The resulting expression is

$$P_{IM} = mP_1 + nP_2 + (T - 28)/10 + B \tag{11}$$

where P_{IM} = power in dBm of the IMP,

P_1 = power in dBm of the input signal at frequency f_1,

P_2 = power in dBm of the input signal at frequency f_2,

T = temperature in degrees Celsius, and

B = -93 dBm with a standard deviation of 6 dB for a MIM junction without sealant

= -72 dBm with a standard deviation of 18 dB for a MIM junction with a sealant.

Even though limited in its description of the IMP behavior of MIM junctions, this model provides a starting point for quantifying the behavior of these types of interference sources. Much more investigation of MIM junctions is needed to carefully quantify their behavior and to define those specific factors which contribute to the IM products.

4.0 MODEL VERIFICATION

The model summarized in the previous section was developed from the measured data on 57 test samples and describes the effects of one test sample parameter (sealant) and four external parameters (vibration, temperature, pressure, and input power) on IMP generation. Other parameters were shown to have no measurable or consistent effect. In order to verify these observations two new test samples were constructed as outlined in Section 3.2 with the material given in Appendix A. In measuring the IMP levels of these verification test samples, vibration, temperature, pressure, input power, and frequency were varied using techniques described in Section 3.3 and Appendix C. Table 4 gives the specific values for each of the external parameters and the measured IMP levels for both verification test samples.

The measured IMP levels for Verification Test Samples #1 and #2 with an input power of +44 dBm, a frequency of 350 MHz, and a temperature of 28° C are well within the range predicted by the model for test samples with a sealant, i.e., -72 dBm with a standard deviation of 18 dB. Furthermore, both verification test samples produced stable IMP levels with vibration having no effect.

The data for temperature versus IMP generation is shown graphically in Figure 11. The model predicts that for every 10° C increase in temperature the IMP level will increase 1 dB. This relationship is not evident in Figure 11. Indeed, the IMP levels tended to decrease as the temperature increases. A re-evaluation of this relationship considering both the original data and the verification data indicates that a change in temperature does cause a change in IMP level; however, the magnitude or direction of this change is not predictable.

Next an external pressure was applied to the verification test samples. For both test samples no effect on IMP levels was observed. Recall that both test samples produced stable IMP levels. Therefore, according to the model no effect was expected.

The data for input power versus IMP levels is shown graphically in Figure 12 for Verification Test Sample #1 and in Figure 13 for Verification Test Sample #2. For both test samples the fundamental input powers were kept

TABLE 4

VERIFICATION OF TEST PARAMETERS, THEIR VALUES, AND MEASURED IMP LEVELS

VERIFICATION TEST SAMPLE #	FREQUENCY (MHz)	APPLIED EXTERNAL PRESSURE (PSI)	TEMPERATURE (°C)	FUNDAMENTAL POWER LEVEL (dBm)	MEASURED IMP LEVEL (dBm)
1	22	0	28	44	-49
1	200	0	28	44	-38
1	275	0	28	44	-41
1	350	0	28	44	-44
1	425	0	28	44	-43
1	1117	0	28	44	-54
1	350	0	28	44	-36
1	350	≤5	28	44	-37
2	350	0	28	44	-47
2	350	≤5	28	44	-47
1	350	0	100	44	-44
1	350	0	90	44	-43
1	350	0	80	44	-44
1	350	0	70	44	-44
1	350	0	60	44	-45
1	350	0	50	44	-44
1	350	0	40	44	-37
1	350	0	30	44	-32
1	350	0	20	44	-23
1	350	0	10	44	-23
2	350	0	90	44	-58
2	350	0	80	44	-50
2	350	0	70	44	-45
2	350	0	60	44	-41
2	350	0	50	44	-44
2	350	0	40	44	-45
2	350	0	30	44	-45
2	350	0	20	44	-43
2	350	0	10	44	-44
1	350	0	28	44	-47
2	350	0	28	41	-56
1	350	0	28	38	-65
1	350	0	28	35	-73
1	350	0	28	32	-82
1	350	0	28	29	-91
2	350	0	28	44	-46
2	350	0	28	41	-55
2	350	0	28	38	-64
2	350	0	28	35	-72
2	350	0	28	32	-81
2	350	0	28	29	-90

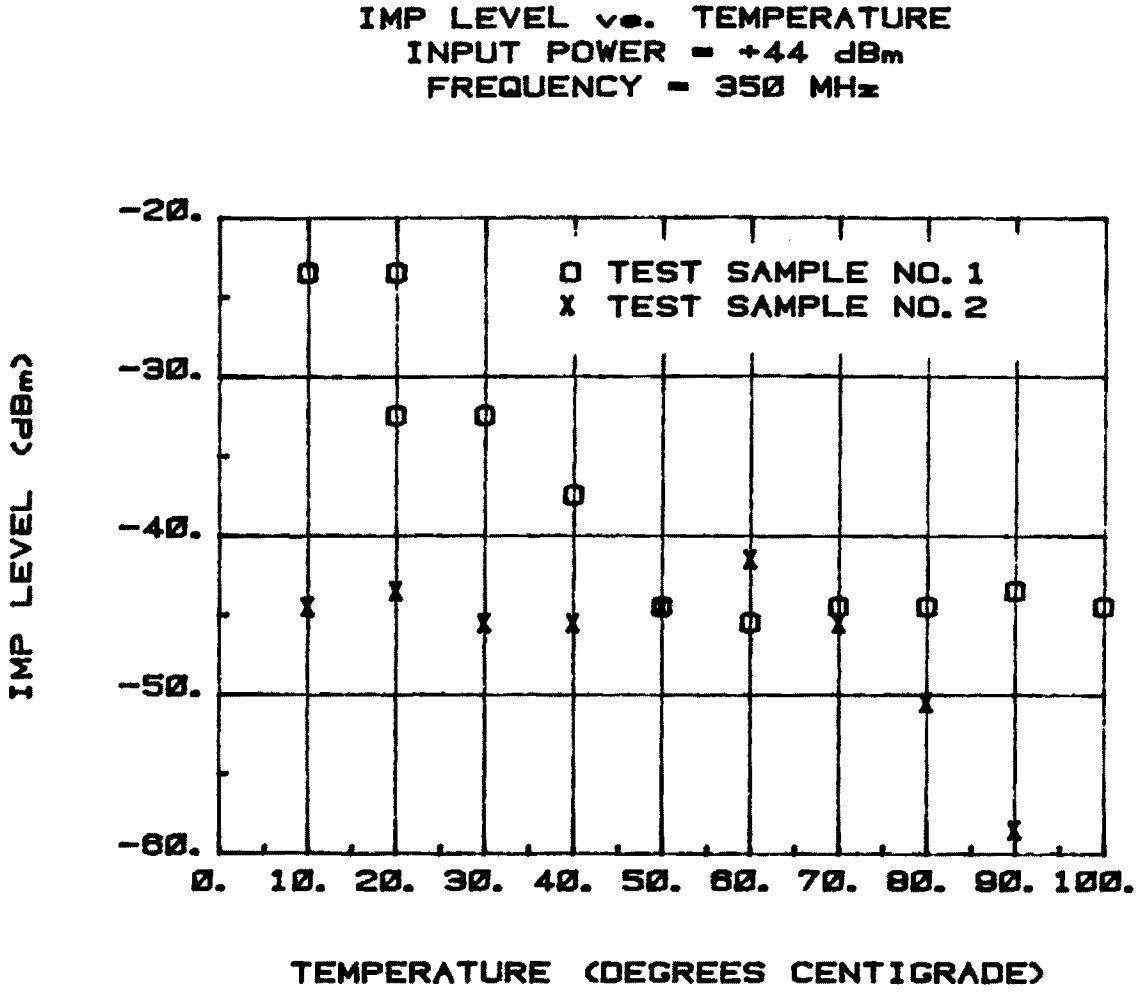

FIGURE 11. IMP LEVEL MEASURED AS A FUNCTION OF TEMPERATURE FOR VERIFICATION TEST SAMPLES NO. 1 AND NO. 2.

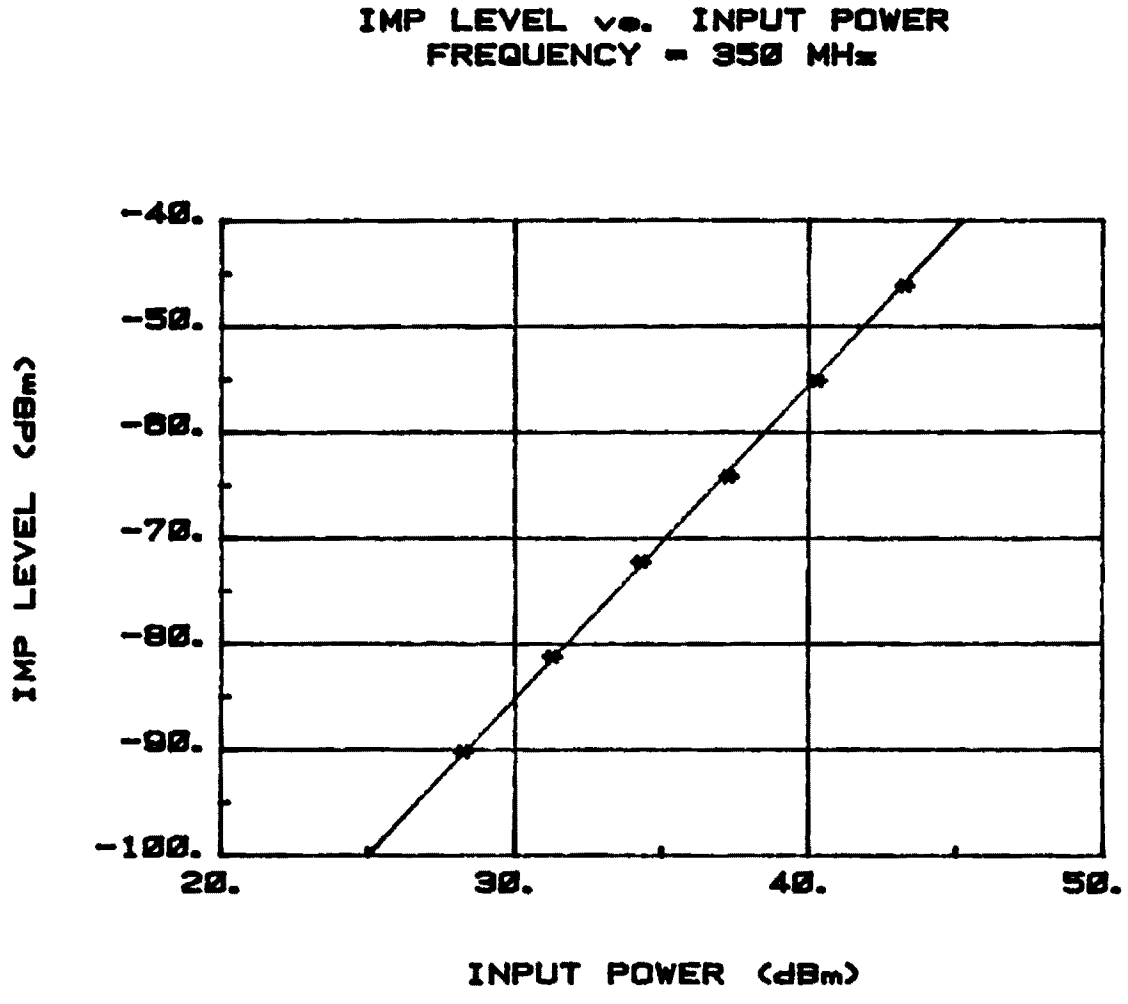

FIGURE 12. IMP LEVEL MEASURED AS A FUNCTION OF INPUT POWER FOR VERIFICATION TEST SAMPLE NO. 1.

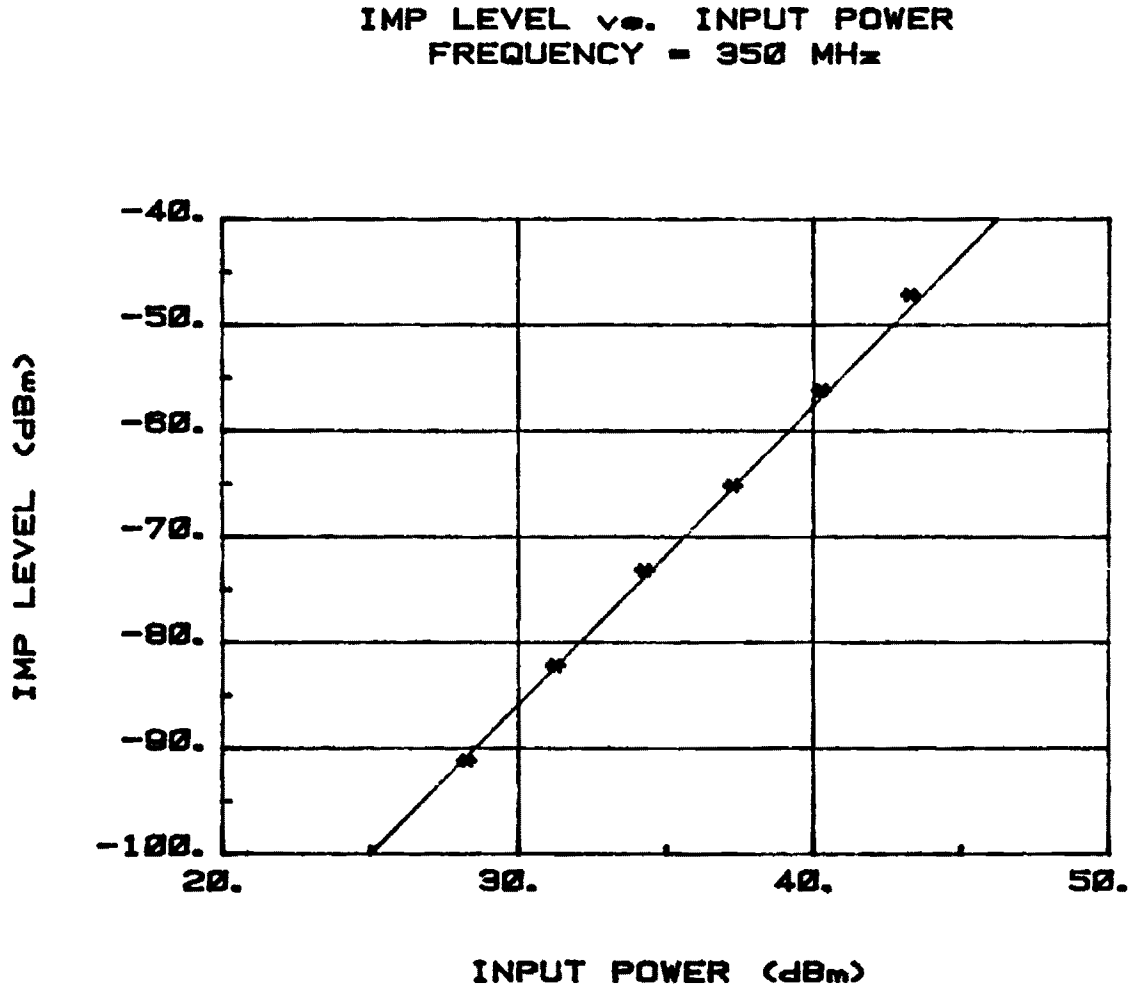

FIGURE 13. IMP LEVEL MEASURED AS A FUNCTION OF INPUT POWER FOR VERIFICATION TEST SAMPLE NO. 2.

equal and both were varied. A slope of 3 is predicted by the model for this case and is plotted with the data. Here the measured data fits very closely with the predicted curve and substantiates the model.

The last external parameter is frequency. The data for frequency versus IMP levels is shown in Figure 14 for Verification Test Sample #1. Again, as for the original data, there is no apparent relationship between frequency and IMP generation.

As a result of these measurements and analysis, each of the relationships in the model was verified except for temperature versus IMP level. The IMP measurements for temperature variations were inconsistent, if not contradictory, to the model predictions. Therefore, the model, Equation (11), in Section 3.4 should be changed to:

$$P_{IM} = m\,P_1 + n\,P_2 + B \qquad (12)$$

where P_{IM} = power in dBm of the IMP,

P_1 = power in dBm of the input signal at frequency f_1,

P_2 = power in dBm of the input signal at frequency f_2, and

B = -93 dBm with a standard deviation of 6 dB for a MIM junction without a sealant

= -72 dBm with a standard deviation of 18 dB for a MIM junction with a sealant.

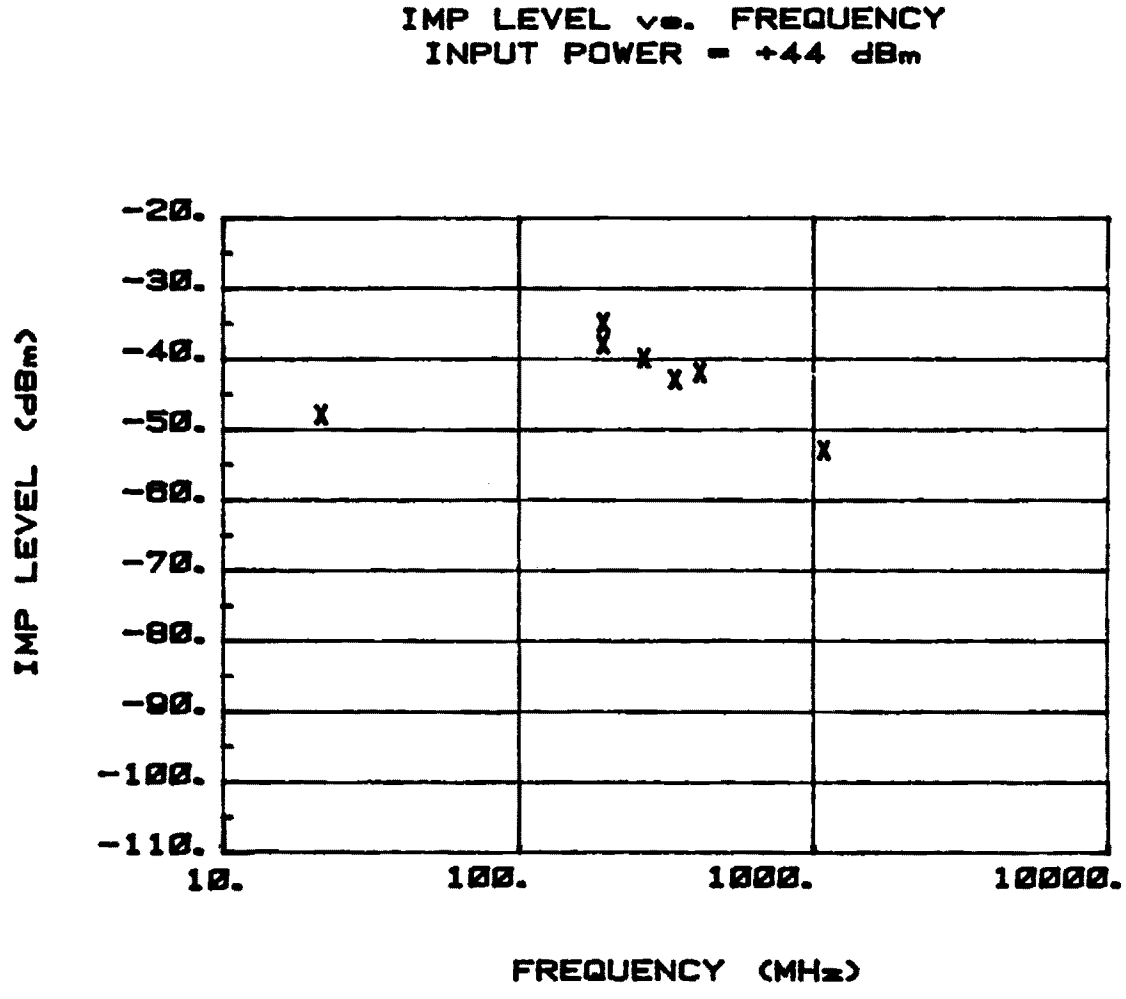

FIGURE 14. IMP LEVEL MEASURED AS A FUNCTION OF FREQUENCY FOR VERIFICATION TEST SAMPLE NO. 1.

5.0 CONCLUSIONS AND RECOMMENDATIONS

Initially an in-depth literature review and analysis was undertaken to determine the feasibility of developing a model based on quantum electron tunneling theory. As a result, it was concluded that a measurement approach was more feasible and appropriate. A sensitive test setup was used which was proven to accurately and repeatably measure the levels of IMPs produced by passive devices. Test samples were then constructed which model MIM junctions as a function of junction parameters. The construction paralleled industrial aircraft construction techniques and used identical materials. In addition, one sample was a panel removed from a typical aircraft. The IMP levels of these test samples were measured at different frequencies, pressures, temperatures, and input power levels. Models were then developed which predict IMP levels from the causative parameters. Finally, the models were verified by measuring the IMP levels of two new test samples and comparing the results to predicted values. The following general conclusions and recommendations resulting from this process are offered:

(1) The literature review revealed that:

- Much research has already been done in this area with large disagreements as to the correct form of the tunneling equations.
- Current state-of-the-art tunneling theory can only predict I-V curves at dc with no frequency dependance.
- Measured I-V curves on carefully controlled idealized MIM junctions, even at dc, are not accurately represented by contemporary electron tunneling models.
- Due to the large number of variables in typical (real-world) MIM junctions and to the inherent instability of the phenomenon, it is the opinion of most researchers that an electron tunneling model cannot predict IMP levels on C^3I platforms.
- If an electron tunneling model were developed, it would at best predict IMP levels only for idealized MIM junctions where each parameter was carefully controlled and measured.
- An empirical model based on measurements of representative MIM junctions has the greatest chance for success.

(2) As a result of the previous conclusions, a measurement scheme was utilized to measure the third order IMPs generated in MIM junctions. Levels ranged from -101 dBm to -31 dBm for an input power of +44 dBm and frequencies between 22 MHz and 1117 MHz. The following general conclusions about the test samples were formulated:

- o MIM junctions can generate IMPs that are significantly higher than IMPs generated by coaxial cables and connectors.
- o The levels of IMPs for some junctions can be very stable. However, most junctions have very unstable IMP levels with a wide range of possible values which, in general, are neither predictable or repeatable.
- o Due to the large variations in IMP levels with no apparent change in the external parameters a theoretical model is difficult to derive.
- o Junction constructed with a typical aircraft sealant generate high IMP levels with larger variations than junctions without a sealant.
- o The behavior of most MIM junctions are very similar to "bad" coaxial cables and connectors.

(3) It was possible to model some of the external causative parameters. The variation of each parameter can be summarized as follows:

- o IMP level is a linear function (in dB) of input power.
- o An increase in external pressure causes a decrease in IMP level to approximately the minimum level for test samples with unstable IMP levels.

(4) It is recommended that further investigations be conducted to determine methods of reducing IMP levels in MIM junctions. Recommended studies include the following:

- o Determine the effect of conductive sealants versus non-conductive sealants.
- o Determine the effect of higher pressure riveted junctions.
- o Compare construction practices and materials between manufacturers and examine their effect on IMP generation.

- Conduct controlled investigations of actual MIM junctions on C^3I aircraft.

- Perform detailed studies on junctions constructed so as to vary only an individual parameter at a time. The number of junctions to be measured should be large enough to statistically define the behavior of IM products with the particular parameters.

6.0 REFERENCES

1. S. M. Perlow, "Third-Order Distortion in Amplifiers and Mixers," RCA Review, Vol. 37, June 1976, pp. 234-266.

2. H. W. Denny, "Linearization Techniques for Broadband Transistor Amplifiers," 1970 IEEE Electromagnetic Compatibility Symposium Record, July 1970, pp. 61-70.

3. D. Kornfield, et al., "Investigation of RFI Due to Nonlinearities in Transistor Amplifiers," 1967 IEEE Electromagnetic Compatibility Symposium Record, July 1967, p. 19.

4. J. L. Allen, "Investigation of Low Level Aircraft Nonavionic Nonlinear Interference," RADC-TR-81-26, Contract No. F30602-78-C-0120, University of South Florida, Tampa, FL, April 1981.

5. J. A. Betts & D. R. Ebenezer, "Intermodulation Interference in Mobile Multiple-Transmission Communication Systems Operating at High Frequencies (3-30 MHz)," Proc. IEEE, Vol. 120, No. 11, Nov. 1973, pp. 1337-1344.

6. R. C. Chapman, J. C. Darlington, A. Savarin, R. Steinberg, A. Paul and R. Moss, "Intermodulation Generation in Normally Passive Linear Components," Philco-Ford Corp. Rep. WDL-TR5242, Aug. 24, 1973.

7. V. Peterson and P. Harris, "Harmonic Testing Pinpoints Passive Component Flaws," Electronics, July 11, 1966, pp. 97-98.

8. N. E. Feldman, et al., Communication Satellites for the 70's: Systems, MIT Press, Cambridge, MA, 1971, p. 375.

9. F. S. McCartney, et al., "FLTSATCOM Program Review: Requirements, Design and Performance," EASCON '78 Record, p. 442.

10. "Report on Electromagnetic Interference problems of SA-5", Electromagnetic Section Engineering Support Division Assistant Director for Instrumentation, IN-K-ES2-64-1, Feb. 14, 1964, J. F. Kennedy Space Center.

11. Chase, W. M., and T. L. Whalen, "Receiving System Intermodulation Interference - An investigation of Typical Devices and a Steel Wire as Sources of RF Interference, NEL Report 1264, U.S. Navy Electronics Laboratory, San Diego, CA 92152.

12. Lustgarten, M. N., "Preliminary Review of 'Rusty Bolt' Phenomena," ECAD-TN-71-18, Electromagnetic Compatibility Analysis Center (ECAC), Annapolis, MD 21402, April 1971.

13. Chase, W. M., et al., "A Method of Control of Shipboard Topside Intermodulation Interference," 1977 IEEE International Symposium on Electromagnetic Compatibility, Seattle, Washington, Aug. 2-4, 1977, pp. 163-165.

14. F. Arazm and F. A. Benson, "Nonlinearities in Metal Contacts at Microwave Frequencies," IEEE Transactions Electromagnetic Compatibility, Vol. EMC-22, No. 3, August 1980, pp. 142-149.

15. F. Matos, "A Brief Survey of Intermodulation Due to Microwave Transmission Components," IEEE Transactions on Electromagnetic Compatibility, Vol. EMC-19, No. 1, February 1977, pp. 33-34.

16. M. B. Amin and F. A. Benson, "Coaxial Cables as Sources of Intermodulation Interference at Microwave Frequencies," IEEE Transactions Electromagnetic Compatibility, Vol. EMC-20, No. 3, August 1978, pp. 376-384.

17. J. C. Lee, "Intermodulation Measurement in the UHF Band and an Analysis of Some Basic Conducting Materials," Technical Note 1979-70, ESD-TR-79-269, Contract No. F19628-80-C-0002, Lincoln Laboratory, Massachusetts Institute of Technology, Lexington, MA, November 1979.

18. J. A. Woody and T. G. Shands, "Investigation of Intermodulation Products Generated in Coaxial Cables and Connectors," Final Report, Contract No. F30602-81-C-0059, Georgia Institute of Technology, Atlanta, GA, May 1982.

19. R. Holm, "The Electric Tunnel Effect across Thin Insulator Films in Contacts," Journal of Applied Physics, Vol. 22, No. 5, May 1951.

20. C. S. Guenzer, "Comments on Spurious Signals Generated by Electron Tunneling on Large Reflector Antennas," Proc. IEEE, Vol. 64, Feb. 1976, p. 283.

21. F. Foriani and N. Minnaja, "Rectification by Means of Metal-Dielectric-Metal Sandwiches," Nuovo Cimento, March 1964, Vol. 31, pp. 1246-1257.

22. R. Stratton, "Volt-current Characteristics for Tunneling Through Insulating Films," J. Phys. Chem. Solids, Vol. 23, 1962, pp. 1177-1190.

23. W. F. Brinkman, R. C. Dynes and J. M. Rowell, "Tunneling Conductance of Asymmetrical Barriers," Journal of Applied Physics, Vol. 41, Apr. 1970, pp. 1915-1921.

24. J. G. Simmons, "Generalized Formula for the Electric Tunnel Effect Between Similar Electrodes Separated by a Thin Insulating Film," Journal of Applied Physics, Vol. 34, June 1963, pp. 1793-1803.

25. R. Holm, Electric Contact: Theory and Application, Springer-Verlag (Berlin), 1967.

26. A Sommerfeld and H. Bethe, Handbuch der Physik von Geiger und Scheel, Vol. 24/2, Julius Springer - Verlag, Berlin, 1933, p. 450.

27. L. I. Schiff, Quantum Mechanics, McGraw-Hill; New York, 1968.

28. C. D. Bond, C. S. Guenzer, and C. S. Carosella, "Generation of Intermodulation by Electron Tunneling through Aluminum Oxide Films," Chapter I of "Studies on the Reduction of Intermodulation Generation in Communication Systems," NRL Memorandum Report 4233, Naval Research Laboratory, Washington, DC, 7 July 1980, AD-E000-492.

29. W. H. Higa, "Spurious Signals Generated by Electron Tunneling on Large Reflector Antennas," Proc. IEEE, Vol. 63, Feb. 1975, pp. 306-313.

30. M. R. McMillan, Nonlinear Junction Characterization, Defense Research Establishment Ottawa (Ontario), May 1979, DREO-TN-79-7.

31. J. G. Simmons, G. J. Unterkofler, and W. W. Allen, "Temperature Characteristics of BeO Tunneling Structures," Journal of Applied Physics, Vol. 2, No. 4, 15 February 1963, pp. 78-80.

32. C. D. Bond, C. S. Guenzer and C. A. Carosella, "Intermodulation Generation by Electron Tunneling Through Aluminum-Oxide Films," Proc. IEEE, Dec. 1979, pp. 1643-1652.

33. J. C. Fisher and I. Giaever, "Tunneling Through Thin Insulating Layers," Journal of Applied Physics, Vol. 32, No. 2, pp. 172-177.

34. H. P. Knauss and R. A. Breslow, "Current-Voltage Characteristics of Tunnel Junctions," Proc. IRE, Vol. 50, Aug. 1962, p. 1843.

35. F. C. McVay, "Don't Guess the Spurious Level," Electronic Design, Vol. 15, No. 3, 1 February 1967, pp. 70-73.

APPENDIX A

TEST SAMPLES

The MIM junction test samples which were used for measurement and modeling of IMP generation were chosen to be representative of the junctions typically found on the fuselage and wings of C^3I aircraft. Because of the large number of such junctions on aircraft, they are probably the major source of IMP generation from aircraft MIM junctions. The test samples were selected so as to vary the material parameters of the MIM junctions. Specifically, the test samples were selected to vary metal type and thickness, chemical treatment, metal primer, sealant, rivet types, and rivet pattern (number and location). In addition, a few test samples of solid metal (i.e., with no MIM junction) and one test sample cut from a panel of a KC-135 aircraft were chosen for comparison. All of the selected test samples and their associated material parameters are identified in Table A-1.

The Test Sample No. in Table A-1 is a number assigned to each test sample in sequential order to aid in keeping track of the test samples during the measurements. The ID No. is an identification number engraved in each test sample as it was constructed. The number in the Aluminum Alloy Type column specifies the characteristics of the aluminum in the test samples as defined in "Aluminum Standards and Data 1979" published by the Aluminum Association, Inc., Washington, DC. Test Samples 50 through 55 were metals other than aluminum; therefore, the specific type of metals for these test samples are given in the Aluminum Alloy Type column.

In addition to untreated, four types of chemical treatments for the surfaces of the metal in the test samples were employed. Some samples were anodized with either chromic or sulfuric acid in accordance with MIL-A-8625* which resulted in coatings with thicknesses of 0.08 to 0.10 mils or 0.30 to 0.50 mils, respectively. Other samples had either color or clear conversion coatings in accordance with MIL-C-5541**.

---

*"Anodic Coatings for Aluminum And Aluminum Alloys," MIL-A-8625, 13 March 1969.

**"Chemical Conversion Coatings on Aluminum And Aluminum Alloys," MIL-C-5541, 14 April 1981.

Similarly, two types of paint primer were used in addition to unpainted metal. Some samples had a zinc chromate primer (TT-P-1757)* with a thickness of 0.30 to 0.40 mils. Other samples had an epoxy polyamide primer (MIL-P-23377)** with a thickness of 0.30 to 0.70 mils.

For the test samples on which a sealant was applied, the sealant consisted of polysulfides (95-97%) with chromate inhibitors (3-5%) and was manganese cured.

Two types of rivets were used: buck and torque controlled. The buck type rivet is inserted through the panels and peaned over. The torque controlled rivet has a nut which only allows a certain amount of torque. When this torque is reached the tightening collar twists off so no further torque can be applied.

Table A-2 contains both verification test samples and their associated material parameters. All of the headings in Table A-2 are the same as in Table A-1 and are discussed above.

---

* "Primer Coatings, Zinc Chromate, Low Moisture Sensitivity," TT-P-1757, 14 August 1972.

** "Primer Coatings Epoxy-Polyamide Chemical and Solvent Resistant," MIL-P-23377, 22 March 1982.

TABLE A-1

TEST SAMPLES

Test Sample No.	ID No.	Aluminum Alloy Type	Nominal Thickness (mils)	Chemical Treatment	Primer Type	Sealant (yes/no)	Rivets	
							Number on Each Side of Junction	Type
1	1	2024-T3-A	63	None	None	Yes	1	Torque
2	2	2024-T3-A	63	None	None	Yes	1	Torque
3 (1)	3	2024-T3-A	63	None	None	No	4	Buck
4	4	2024-T3-A	63	Chromic Acid Anodized	Zinc Chromate	Yes	1	Torque
5	5	2024-T3-A	63	Chromic Acid Anodized	Epoxy Polyamide	Yes	1	Torque
6	6	2024-T3-A	63	Sulfuric Acid Anodized	Zinc Chromate	Yes	1	Torque
7	7	2024-T3-A	63	Sulfuric Acid Anodized	Epoxy Polyamide	Yes	1	Torque
8	8	2024-T3-A	63	Color Conversion Coating	Zinc Chromate	Yes	1	Torque
9	10	3003-H-14	30	None	None	No	1	Torque
10	11	3003-H-14	40	None	None	No	1	Torque

(continued)

TABLE A-1 (continued)

TEST SAMPLES

Test Sample No.	ID No.	Aluminum Alloy Type	Nominal Thickness (mils)	Chemical Treatment	Primer Type	Sealant (yes/no)	Rivets	
							Number on Each Side of Junction	Type
11	12	3003-H-14	125	None	None	No	1	Torque
12	13	6061-T6	40	None	None	No	1	Torque
13	14	6061-T6	50	None	None	No	1	Torque
14	15	6061-T6	125	None	None	No	1	Torque
15	16	7075-T6-A	40	Chromic Acid Anodized	None	No	1	Torque
16	17	7075-T6-A	40	Chromic Acid Anodized	Zinc Chromate	Yes	1	Torque
17	18	7075-T6-A	40	Chromic Acid Anodized	Epoxy Polyamide	Yes	1	Torque
18	19	7075-T6-A	40	Sulfuric Acid Anodized	Zinc Chromate	Yes	1	Torque
19	20	7075-T6-A	40	Sulfuric Acid Anodized	Epoxy Polyamide	Yes	1	Torque

(continued)

TABLE A-1 (continued)

TEST SAMPLES

Test Sample No.	ID No.	Aluminum Alloy Type	Nominal Thickness (mils)	Chemical Treatment	Primer Type	Sealant (yes/no)	Rivets	
							Number on Each Side of Junction	Type
20	21	7075-T6-A	40	Color Conversion Coating	None	No	1	Torque
21	22	7075-T6-A	40	Color Conversion Coating	Zinc Chromate	Yes	1	Torque
22	23	7075-T6-A	40	Color Conversion Coating	Epoxy Polyamide	Yes	1	Torque
23	24	7075-T6-A	40	Clear Conversion Coating	None	No	1	Torque
24	25	7075-T6-A	40	Clear Conversion Coating	Zinc Chromate	Yes	1	Torque
25	26	7075-T6-A	40	Clear Conversion Coating	Epoxy Polyamide	Yes	1	Torque
26	27	7075-T6-B	80	Chromic Acid Anodized	None	No	1	Torque
27	28	7075-T6-B	80	Chromic Acid Anodized	Zinc Chromate	Yes	1	Torque

(continued)

TABLE A-1 (continued)

TEST SAMPLES

Test Sample No.	ID No.	Aluminum Alloy Type	Nominal Thickness (mils)	Chemical Treatment	Primer Type	Sealant (yes/no)	Rivets	
							Number on Each Side of Junction	Type
28	29	7075-T6-B	80	Chromic Acid Anodized	Epoxy Polyamide	Yes	1	Torque
29	30	7075-T6-B	80	Sulfuric Acid Anodized	None	Yes	1	Torque
30	32	7075-T6-B	80	Sulfuric Acid Anodized	Epoxy Polyamide	Yes	1	Torque
31	33	7075-T6-B	80	Color Conversion Coating	None	Yes	1	Torque
32	34	7075-T6-B	80	Color Conversion Coating	Zinc Chromate	Yes	1	Torque
33	35	7075-T6-B	80	Color Conversion Coating	Epoxy Polyamide	Yes	1	Torque
34	36	7075-T-6511-X	63	None	None	No	1	Torque
35	37	7075-T-6511-X	100	None	None	No	1	Torque
36	38	7075-T6-A	40	Sulfuric Acid Anodized	None	No	1	Buck

(continued)

TABLE A-1 (continued)

TEST SAMPLES

Test Sample No.	ID No.	Aluminum Alloy Type	Nominal Thickness (mils)	Chemical Treatment	Primer Type	Sealant (yes/no)	Rivets	
							Number on Each Side of Junction	Type
37	41	7075-T6-B	80	None	None	No	1	Torque
38	42	7075-T6-B	80	None	None	Yes	1	Torque
39	43	7075-T6-B	80	None	None	Yes	1	Torque
40	44	2024-T3-A	63	None	None	No	4	Buck
41	45	2024-T3-A	63	None	None	No	4	Buck
42	46	2024-T3-A	63	None	None	No	4	Buck
43	47	2024-T3-A	63	None	None	No	3	Buck
44	48	2024-T3-A	63	None	None	No	1	Buck
45	49	2024-T3-A	63	None	None	No	1	Torque
46	50	(Note 2)	63	?	?	?	?	?
47	51	7075-T6-A	40	Sulfuric Acid Anodized	None	Yes	1	Torque
48	52	7075-T6-A	40	Sulfuric Acid Anodized	None	Yes	1	Torque

(continued)

TABLE A-1 (concluded)

TEST SAMPLES

Test Sample No.	ID No.	Aluminum Alloy Type	Nominal Thickness (mils)	Chemical Treatment	Primer Type	Sealant (yes/no)	Rivets	
							Number on Each Side of Junction	Type
49	53	2024-T3-A	63	None	None	No	(Note 3)	--
50	100	Copper[4]	63	None	None	No	(Note 5)	--
51	110	Copper[4]	63	None	None	No	1	Buck
52	120	Tin[4]	24	None	None	No	(Note 5)	--
53	130	Tin[4]	24	None	None	No	1	Buck
54	140	Brass[4]	63	None	None	No	(Note 5)	--
55	150	Brass[4]	63	None	None	No	1	Buck
56	180	2024-T3-A	63	None	None	No	(Note 5)	--
57	190	2024-T3-A	63	None	None	No	(Note 5)	--

Notes:
1. This test sample was weathered by placing it outside for one month.
2. This test sample was constructed from a section of a KC-135 aircraft fuselage. Since the junction was already in the section of fuselage, the material properties of the junction are unknown.
3. The junction in this test sample was clamped together with wooden strips and rubber bands.
4. These test samples were constructed with the types of metal indicated and not with aluminum alloys. The copper indicated is drawn copper while the tin is tin plate.
5. These test samples consist of solid pieces of metal with no junction.

TABLE A-2

VERIFICATION TEST SAMPLES

Verification Test Sample No.	ID No.	Aluminum Alloy Type	Nominal Thickness (mils)	Chemical Treatment	Primer Type	Sealant (yes/no)	Number on Each Side of Junction	Type
1	9	2024-T3-A	63	Color Conversion	Epoxy	Yes	1	Torque
2	31	7075-T6-B	80	Sulfuric Acid Chromate	Zinc Chromate	Yes	1	Torque

APPENDIX B

IMP MEASUREMENT SCHEME

A repeatable, accurate, and sensitive measurement scheme for use in collecting data to characterize the IMPs generated in passive devices was developed on a recent RADC effort*. On that effort, test setups for IMP frequencies of 22 MHz and 200 to 425 MHz were developed. Based on the same measurement scheme, a test setup for an IMP frequency of 1117 MHz was developed on the current program. The general arrangements of all these test setups are identical. A block diagram of the test setups is given in Figure B-1. A few changes in specific components were necessary as a result of the changes in frequencies. The equipment and components employed in each test setup are identified in Table B-1. Descriptions of the test setups as well as their differences are summarized in this appendix. The block diagram in Figure B-1 illustrates that the test setup consists of three major sections: (1) the Power Source/Combiner Section, (2) the Test Sample Section, and (3) the Load/Detector Section. The purposes of the Power Source/Combiner Section are to (1) generate the required levels of RF power at the fundamental frequencies, (2) combine these two fundamental signals so that they can be applied to the test samples, and (3) monitor the input power levels to the test samples. The power combiner in Table B-1 for 22 MHz consists of two Pi-network impedance transformers with a common output as illustrated in Figure B-2. (This figure also shows the interconnection of the power combiner with the other elements of the Power Source/Combiner Section of the test setup.) The characteristic impedance of the transformers is 50 ohms such that their output impedances, $Z_{out}(f)$ are given by

$$Z_{out} = \frac{(50)^2}{Z_B} \qquad \text{(B-1)}$$

*J. A. Woody and T. G. Shands, "Investigation of Intermodulation Products Generated in Coaxial Cables and Connectors," RADC-TR-82-240 Final Report, Contract No. F30602-81-C-0059, Georgia Institute of Technology, Atlanta, GA, September 1982.

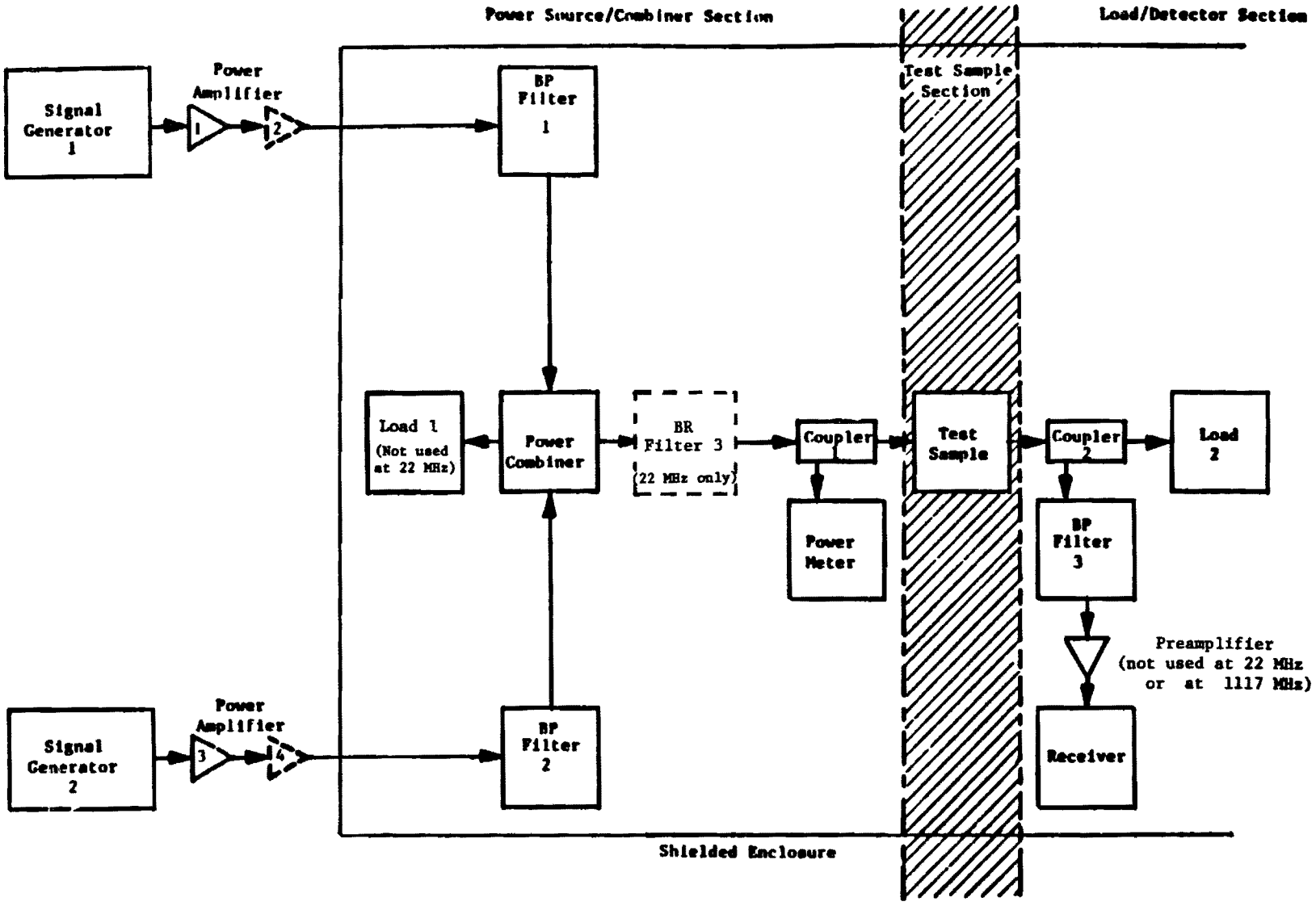

Figure B-1. Measurement Setup.

TABLE B-1

COMPONENTS OF THE TEST SETUP

Test Setup Section	Test Setup Component	Component Description		
		22-MHz Setup	200 to 425-MHz Setup	1117-MHz Setup
Power Source/ Combiner	Signal Generator 1	HP 8640B Signal Generator	HP 8640B Signal Generator	HP 8640B Signal Generator
	Signal Generator 2	HP 8640B Signal Generator	HP 8640B Signal Generator	HP 8640B Signal Generator
	Power Amplifier 1	AILTECH 5020 Broadband Amplifier	AILTECH 20512 Broadband Amplifier	AILTECH 15100B Broadband Amplifier
	Power Amplifier 2*	Drake L-4B Linear Amplifier	ARCOS UHF-500 Power Amplifier	(Not used)
	Power Amplifier 3	Amplifier Research 100L Broadband Amplifier	AILTECH 35512 Broadband Amplifier	AILTECH 15100B Broadband Amplifier
	Power Amplifier 4*	Heathkit SB-221 Linear AMplifier	ARCOS UHF-500 Power Amplifier	(Not used)
	BP Filter 1	Bandpass Filter --Helical Resonator tuned to 17.88 MHz	Bandpass Filter --Single tuned, high Q cavity resonator (218 to 400 MHz)	Bandpass Filter --High Q cavity resonator (1036.28 MHz)

(continued)

TABLE B-1 (continued)

COMPONENTS OF THE TEST SETUP

Test Setup Section	Test Setup Component	Component Description		
		22-MHz Setup	200 to 425-MHz Setup	1117-MHz Setup
	BP Filter 2	Bandpass Filter --Lumped-constant filter tuned to 19.89 MHz	Bandpass Filter --Collins 156C-2 multicoupler (220 to 400 MHz)	Bandpass Filter --High Q cavity resonator (955.47 MHz)
	BR Filter 3	Band-reject Filter --Lumped-constant filter tuned to 21.9 MHz	(Not used)	(Not used)
	Power Combiner	Two Pi-network Impedance Transformers with a common output	Stripline Hybrid (see text)	Stripline Hybrid (see text)
	Load 1	(Not used)	250-ft length of RG-223/U with a 50-ohm termination	250-ft length of RG-223/U with a 50-ohm termination
	Coupler 1	Narda 3020 Bi-Directional Coupler with 50-ohm termination on reverse port	Narda 3020 Bi-Directional Coupler with 50-ohm termination on reverse port	Narda 3020 Bi-Directional Coupler with 50-ohm termination on reverse port
	Power Meter	HP 435A Power Meter	HP 435A Power Meter	HP 435A Power Meter

(continued)

TABLE B-1 (concluded)

COMPONENTS OF THE TEST SETUP

Test Setup Section	Test Setup Component	Component Description		
		22-MHz Setup	200 to 425-MHz Setup	1117-MHz Setup
Load/Detector	Coupler 2	HP 778D Dual Directional Coupler (or Narda 3020A Bi-Directional Coupler)* with 50-ohm termination on reverse port	HP 778D Dual Directional Coupler (or Narda 3020A Bi-Directional Coupler)* with 50-ohm termination on reverse port	HP 778D Dual Directional Coupler (or Narda 3020A Bi-Directional Coupler)* with 50-ohm termination on reverse port
	Load 2	Bird Termaline 8251 Coaxial Resistor	Bird Termaline 8251 Coaxial Resistor	Bird Termaline 8251 Coaxial Resistor
	BP Filter 4	Two Bandpass Filters--Lumped-constant filters tuned to 21.9 MHz	Telonic TTF190-5-5EE or Telonic TTA375-3-5EE Tunable Bandpass Filter	Bandpass Filter High Q Cavity Resonator (1117.09 MHz)
	Preamplifier	(Not used)	Miteq AM-3A-000110 Preamplifier	Miteq AM-3A-000110 Preamplifer
	Receiver	HP 141T Spectrum Analyzer with HP 8554L RF Section and HP 8552B IF Section	HP 141T Spectrum Analyzer with HP 8554L IF Section and HP 8552B IF Section	HP 141T Spectrum Analyzer with HP 8554L RF Section and HP 8552B IF Section

*Used for input powers greater than 44 dBm.

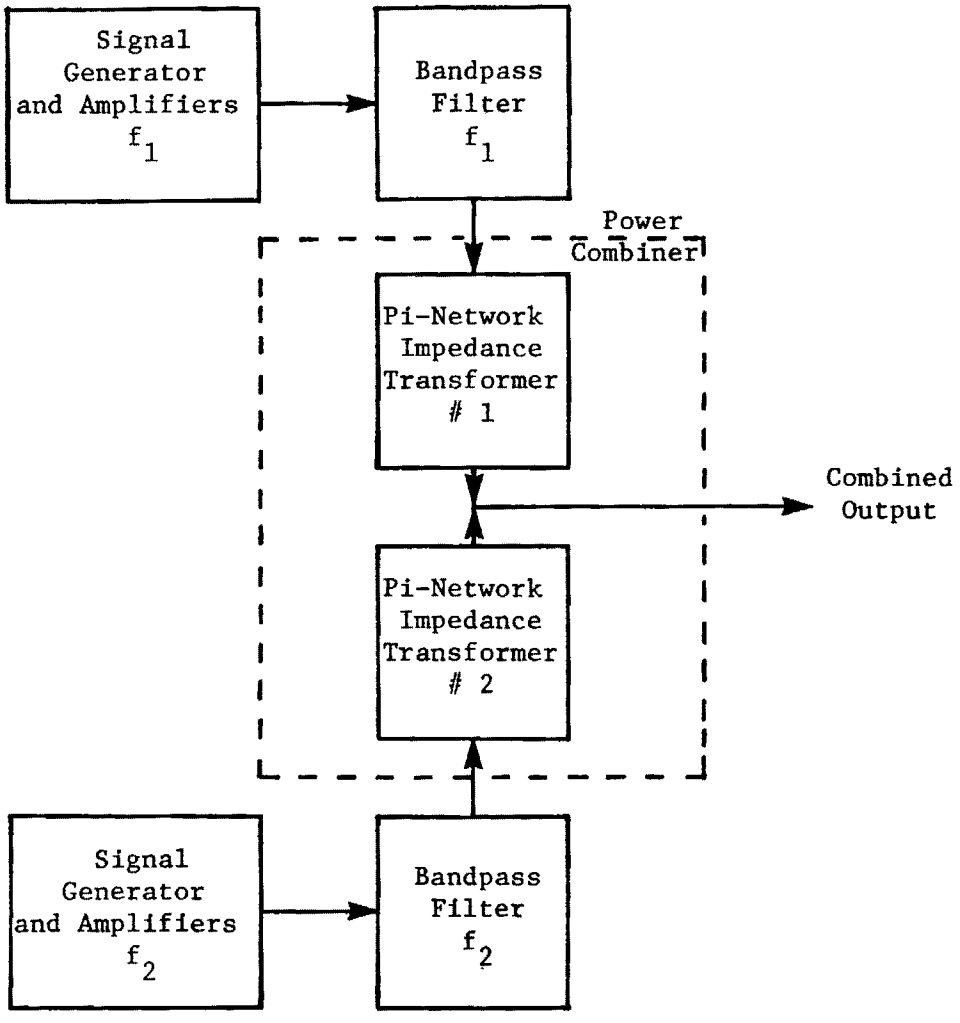

Figure B-2. 22-MHz Power Combiner.

where Z_B is the frequency dependent output impedance of the bandpass filter. At frequency f_1, the output impedance, Z_{B1}, of the bandpass filter for f_1 is 50 ohms. Hence, from Equation (B-1) the output impedance of Pi-network #1 at f_1 is 50 ohms. Also, at frequency f_1, the output impedance of the bandpass filter for f_2 is very low; therefore, again from Equation (B-1), the output impedance of Pi-network #2 at f_1 is very high. Hence, very little of the f_1 signal couples through Pi-network #2 and the bandpass filter for f_2. The output impedance of the power combiner at frequency f_1 is essentially 50 ohms (from Pi-network #1) in parallel with a very high impedance (from Pi-network #2) or is approximately 50 ohms. Thus, essentially all of the signal at f_1 is coupled to the combined output port. At frequency f_2 the roles of Pi-network #1 and bandpass filter for f_1 interchange with those of Pi-network #2 and bandpass filter for f_2. Hence, very little of the signal at f_2 couples to the signal generator and amplifiers for f_1 and essentially all of the f_2 signal appears at the output of the power combiner. In summary, the Power Combiner helps isolate the two fundamental signals and combines them at a common output with very little loss.

The 200 to 425-MHz and the 1117-MHz power combiners consist of stripline hybrids specifically designed for each pair of fundamental frequencies on the previous program. The two input ports to each hybrid were chosen to provide maximum isolation between the fundamental signals and the output port was chosen to give the least insertion loss. The fourth port was terminated in a 50-ohm load. It was noted that an extremely linear load for this port was important in reducing the inherent IMP level of the test setup. A 250-ft length of RG-223/U coaxial cable with a 50-ohm termination was found to provide the necessary linearity.

During the development of the measurement scheme and test setups on the previous effort, it was noted that the inherent IMP level of the 22-MHz setup was excessively high when compared with the test setups for the higher frequencies. Therefore, it was necessary to use a band-reject (i.e., notch) filter in the 22-MHz test setup prior to the test sample. This filter which had an attenuation of 60 dB at the IMP frequency was placed at the output of the power combiner as shown in Figure B-1.

The final components of the Power Source/Combiner Section are a directional coupler and a power meter. They sample the fundamental signal

levels at the input of the test sample, and thus, provide a means of continuously monitoring these signals.

The Test Sample Section of the test setup consists of only the test sample, i.e., a MIM junction mounted in the test jig. The test sample is located between the Power Source/Combiner and Load/Detector Sections of the test setup and is connected to the output of the signal combiner.

The Load/Detector Section of the test setup is connected to the output of the test sample. The purpose of this section is to provide an appropriate termination, i.e., 50-ohm load, for the test sample and to provide a means of detecting the IMPs and measuring their levels. Between the test sample and the load, a directional coupler is used to sample the generated IMP for detection with the receiver. This directional coupler and the two IMP bandpass filters are used to attenuate the two fundamental frequency signals so that they do not create IMPs in the receiver. Except at 22 MHz, a low noise figure (2 dB), high gain (36 dB) preamplifier was used at the input of the receiver. (It could not be employed in the 22-MHz test setup because the resulting amplified fundamental signals produced IMPs in the receiver.) This preamplifier improved the measurement sensitivity of the higher frequency test setups by more than 20 dB.

As shown in Figure B-1, part of the Power Source/Combiner Section and all of the Test Sample and Load/Detector Sections are located inside a shielded enclosure. Specifically, the high power signal sources are located outside the shielded enclosure and the test sample and detection systems are located inside the enclosure. Thus, the enclosure wall provides isolation between the high level signals and the sensitive parts of the test setup. A high degree of isolation was necessary to prevent undesired coupling within the test setup.

APPENDIX C

TEST PROCEDURES

The purpose of this appendix is to outline the basic test procedures followed in measuring a test sample. In general, the test procedures include three basic, sequential steps: (1) calibrate the test setup, (2) prepare the test sample and set the input power levels, and (3) measure the level of the IMPs generated by the test sample.

After the test setup has been configured according to Appendix B, the Power Source/Combiner and Load/Detector Sections are calibrated. A calibrated signal at the frequency of each fundamental is applied to the input of the dual directional coupler in the Power Source/Combiner Section (see Figure B-1). The power level at this point is the same as at the input of the test sample because the insertion loss of the directional coupler is significantly less than 1 dB. The level of each signal is then read on the power meter. The difference between the two input levels and the two measured levels are Calibration Factors 1 and 2. These calibration factors are then added to the power meter readings to determine the power level of each fundamental signal at the input of the test sample. The Load/Detector Section is similarly calibrated by applying a signal at the frequency of the IMP to the input of this section which is normally the output of the Test Sample Section (see Figure B-1). The level at the receiver is then measured. The difference between the input level and the measured level is Calibration Factor 3. This calibration factor is then added to the measured IMP level at the receiver to obtain the actual level of the IMP generated in the test sample. Typical values for all of these calibration factors at each frequency are given in Table C-1.

The test samples are prepared according to Appendix A. The test setup is connected without a test sample. Using Calibration Factors 1 and 2, the power level of each fundamental signal is set equal to the desired level as indicated by the power meter.

To measure the test sample, the receiver (spectrum analyzer) is tuned to the IMP frequency and adjusted for maximum sensitivity (i.e., 300 Hz bandwidth and 10 Hz video filter). The inherent IMP level of the test setup is measured using Calibration Factor 3. This inherent IMP level is then recorded along

TABLE C-1

CALIBRATION FACTORS

Nominal IMP Frequency (MHz)	Calibration Factor 1 (dB)	Calibration Factor 2 (dB)	Calibration Factor 3 (dB)
22	36.0	36.2	37.0
200	20.5	20.0	-14.0*
275	20.5	20.0	-14.2*
350	19.5	19.4	-14.1*
425	19.5	19.4	-14.0*
1117	19.6	20.1	23.5

*These calibration factors are negative because a pre-amplifier was used.

with the input power levels for the two fundamentals, the frequency of the IMP, and the various test sample parameters. The RF power of each signal source is then turned off and a test sample is inserted in the test setup. The mating surfaces of the connectors on the test jig are coated with a silver based conductive grease (Tecknit P/N 72-00016) and securely tightened with hand tools. The RF sources are turned on and the level of the IMP is observed on the receiver. If the IMP level is stable, it is measured using Calibration Factor 3 and recorded. After stable IMP levels are measured or if the observed level is unstable, the test jig and the test setup near the test jig are tapped lightly to determine the effects of vibration on the level of the IMP. The resulting levels are measured using Calibration Factor 3 and recorded. All of the recorded values are given in Appendix D.

This procedure is repeated, except for calibration of the test setup, for all of the test samples in Appendix A. For several test samples, measurements on the same sample are repeated a sufficient number of times to insure that the measured data is a result of the test sample and is not caused by a bad connection of the test sample to the test jig or of the test jig to the remainder of the test setup.

For each new IMP frequency the test setup is prepared according to Appendix B and the entire procedure repeated.

APPENDIX D

MEASURED IMP DATA

The IMP data measured for metal-insulator-metal junctions are listed in Tables D-1 through D-4. Table D-1 presents the data measured for all the test samples at an IMP frequency of 350 MHz and an input power of 44 dBm. Each test sample was measured as many times as its Test Sample No. is listed. A range for the measured IMP level indicates that the measured level was not stable but randomly varied between the two levels given. Table D-2 shows the variation in IMP level as a function of the junction temperature for Test Sample No. 30. Table D-3 presents the variation in IMP level for Test Sample No. 30 with fundamental power levels. The entries in both Tables D-2 and D-3 are listed in the sequence in which they were measured.

Finally, Table D-4 lists the variation of IMP level with the IMP test frequency for three different test samples. In this table, the levels for an IMP frequency of 350 MHz are repeated from Table D-1 for completeness.

TABLE D-1

MEASURED IMP LEVEL FOR EACH TEST SAMPLE WITH INPUT POWER OF 44 dBm AND IM FREQUENCY OF 350 MHz

Test Sample No.	IMP Level (dBm)	Test Sample No.	IMP Level (dBm)
1	-74 to -54	16	-70
2	-101	17	-94 to -54
2	-100	17	-79
2	-85 to -50	18	-94 to -72
2	-104 to -74	18	-104 to -74
3	-89	19	-76
3	-100	20	-94 to -84
3	-90	21	-84
4	-104	21	-89 to -79
4	-79 to -69	22	-54
4	-101	23	-94
4	-55	24	-104 to -94
4	-51	24	-64 to -44
4	-104 to -80	25	-72
5	-102 to -94	25	-72
5	-104 to -74	25	-67
5	-101	26	-100 to -84
5	-59	27	-94 to -64
6	-59	27	-94 to -67
6	-57	28	-104 to -80
6	-46	28	-90 to -68
6	-42	29	-104 to -84
7	-94 to -34	30	-35
7	-61	30	-35
8	-90 to -88	30	-36
8	-94 to -84	30	-32
9	-94 to -84	30	-35
10	-104 to -84	30	-37
11	-98 to -84	30	-34
12	-86	30	-36
13	-104 to -74	30	-37
13	-101	30	-36
13	-104 to -99	30	-32
13	-104 to -99	30	-35
14	-84 to -76	30	-32
15	-91 to -84	30	-31

(Continued)

TABLE D-1 (concluded)

MEASURED IMP LEVEL FOR EACH TEST SAMPLE WITH INPUT POWER OF 44 dBm AND IM FREQUENCY OF 350 MHz

Test Sample No.	IMP Level (dBm)	Test Sample No.	IMP Level (dBm)
31	-99 to -89	46	-104 to -74
32	-104 to -84	47	-80
33	-98	48	-96 to -84
34	-97 to -87	49	-104 to -64
35	-94 to -79	50	-101
36	-104 to -90	50	-102
36	-100	50	-102
36	-100	51	-103
36	-84	51	-102
36	-81	51	-100
37	-94 to -58	51	-92
37	-84	52	-87
38	-104 to -84	52	-88
39	-99 to -84	53	-86
40	-104 to -84	53	-88 to -80
41	-104 to -64	54	-104
42	-104 to -94	54	-84 to -79
43	-92	54	-101
43	-97	54	-97
43	-100	54	-100
43	-104	54	-100
44	-104 to -84	55	-98
45	-97	55	-97
45	-97	55	-101
45	-98	56	-99
45	-84	56	-104
45	-101	56	-104
45	-100	56	-99
45	-104	56	-100
45	-104 to -84	57	-101
45	-101	57	-101
45	-103	57	-101
45	-84	57	-100
45	-94	57	-84
46	-104 to -74	57	-103 to -99

TABLE D-2

MEASURED IMP LEVELS AT DIFFERENT JUNCTION TEMPERATURES FOR TEST SAMPLE NO. 30 AT IM FREQUENCY OF 350 MHz AND INPUT POWER OF 44 dBm

Junction Temperature (°C)	IMP Level (dBm)
28	-34
58	-40
45	-42
40	-42
38	-42
32	-42
30	-42
62	-39
42	-42
9	-44
12	-44
15	-43
18	-43
20	-43
22	-43
26	-43
28	-43
28	-30*
28	-31*
74	-52
30	-49
100	-30
60	-32
50	-34
45	-36
34	-38
60	-34
90	-29

*Between these two measurements, the test sample was removed from the test jig. The remainder of the data was measured the next day.

TABLE D-3

MEASURED IMP LEVELS AT DIFFERENT FUNDAMENTAL POWER LEVELS FOR TEST SAMPLE NO. 30 AT IM FREQUENCY OF 350 MHz

FUNDAMENTAL POWER LEVELS		
Source 1 at 375 MHz (dBm)	Source 2 at 400 MHz (dBm)	IMP Level (dBm)
37.0	41.0	-40.8
39.0	41.0	-38.1
41.0	41.0	-35.8
41.0	41.0	-35.8
36.0	36.0	-41.6
34.0	36.0	-46.6
32.0	36.0	-51.2
30.0	36.0	-54.4
28.0	36.0	-58.2
26.0	36.0	-62.4
36.0	36.0	-41.8
36.0	34.0	-44.2
36.0	32.0	-45.8
36.0	30.0	-47.6
36.0	28.0	-49.5
36.0	26.0	-51.2
36.0	36.0	-41.6
34.0	34.0	-47.6
32.0	32.0	-53.2
30.0	30.0	-58.0
28.0	28.0	-63.6
26.0	26.0	-69.4
41.0	41.0	-36.2
41.0	41.0	-43.8

(Continued)

TABLE D-3 (concluded)

MEASURED IMP LEVELS AT DIFFERENT FUNDAMENTAL POWER LEVELS FOR TEST SAMPLE NO. 30 AT IM FREQUENCY OF 350 MHz

FUNDAMENTAL POWER LEVELS		
Source 1 at 375 MHz (dBm)	Source 2 at 400 MHz (dBm)	IMP Level (dBm)
43.2	41.0	-40.0
45.1	41.0	-36.0
46.8	41.0	-32.8
49.5	41.0	-32.4
47.0	41.0	-38.4
45.0	41.0	-43.0
43.0	41.0	-46.2
41.0	41.0	-50.8
41.0	41.0	-52.0
41.0	43.0	-50.4
41.0	45.0	-47.6
41.0	49.0	-42.0
41.0	41.0	-57.0
44.0	44.0	-47.8
47.0	47.0	-72.0*
41.0	41.0	-70.0*
47.0	47.0	-60.0*
49.0	49.0	-54.0*
44.0	44.0	-94 to -74**

*These numbers are the inherent IMP levels of the test setup at the indicated fundamental power levels.

**The measured IMP level was not stable; it varied between -94 and -74 dBm.

TABLE D-4

MEASURED IMP LEVELS AT DIFFERENT IM TEST FREQUENCIES FOR THREE TEST SAMPLES WITH INPUT POWER OF 44 dBm

TEST SAMPLE NO.	NOMINAL IM FREQUENCY (MHz)	IMP LEVEL (dBm)
4	22	-62
4	200	-93 to -74
4	275	-95 to -79
4	275	-96
4	350	-104
4	350	-79 to -69
4	350	-101
4	350	-55
4	350	-51
4	350	-104 to -80
4	425	-54 to -44
4	1117	75 to -70
6	22	-35
6	200	-58
6	275	-46
6	275	-48
6	350	-59
6	350	-57
6	350	-46
6	350	-42
6	425	-49
6	1117	-44
30	22	-44 to -30
30	200	-48
30	275	-48
30	275	-48
30	350	-35
30	350	-35
30	350	-36
30	350	-32
30	350	-35
30	350	-37
30	350	-34
30	350	-36
30	350	-37
30	350	-36
30	350	-32
30	350	-35
30	350	-32
30	350	-31
30	425	-30
30	425	-29
30	1117	-35

MISSION
of
Rome Air Development Center

RADC plans and executes research, development, test and selected acquisition programs in support of Command, Control Communications and Intelligence (C^3I) activities. Technical and engineering support within areas of technical competence is provided to ESD Program Offices (POs) and other ESD elements. The principal technical mission areas are communications, electromagnetic guidance and control, surveillance of ground and aerospace objects, intelligence data collection and handling, information system technology, ionospheric propagation, solid state sciences, microwave physics and electronic reliability, maintainability and compatibility.